e-ISSN: 3061-9629

2 cilt volume 2 sayı issue 2025 Temmuz July

HITIT JOURNAL OF SCIENCE

HİTİT ÜNİVERSİTESİ YAYINLARI

HİTİT JOURNAL OF SCIENCE

e-ISSN: 3061-9629
Volume: 2 • Issue: 2 - July 2025
Period: 2 Issues per Year (January & July)

LANGUAGE OF PUBLICATION
English

CONTACT ADDRESS
Hitit Üniversitesi Fen Edebiyat Fakültesi, ÇORUM, TÜRKİYE
Tel: +90 364 222 11 00 Fax: +90 364 222 11 02
hjs@hitit.edu.tr | https://dergipark.org.tr/tr/pub/hjs

PUBLISHER
Hitit University Press

HAKEM KURULU | REFEREE BOARD

Hitit Medical Journal Dergisi, çift taraflı kör hakemlik sistemi kullanmaktadır. Hakem isimleri gizli tutulmakta ve yayımlanmamaktadır.

Hitit Medical Journal uses a double-blind review. Referee names are kept strictly confidential.

LOCKSS: https://dergipark.org.tr/tr/pub/hjs/lockss-manifest

OAI: https://dergipark.org.tr/api/public/oai/hjs/

BOARD OF EDITORS

Editörden

Değerli Okuyucular;
Hitit Journal of Science 2025 yılının ikinci sayısı ile sizlerle buluşmaktan büyük bir mutluluk duyuyoruz. Dergimize olan ilgi ve destek için teşekkür ederiz.
Dergimizde, Temel Bilimler (Fizik, Kimya, Biyoloji ve Matematik) alanında kapsamlı ve çeşitli makaleler yayımlamaya özen gösteriyoruz. Bu sayıda da bilim dünyasına katkı sağlayacak 4'ü araştırma makalesi olmak üzere toplam 5 makaleyi siz değerli okuyucularımızla paylaşmanın gururunu yaşıyoruz.
Tüm okuyucularımıza keyifli ve verimli okumalar diliyoruz.
Saygılarımızla,

Prof. Dr. Dursun Ali KÖSE
HJS Editöryal Kurul adına

From the Editor

Dear Readers;

Hitit Journal of Science is very pleased to meet you with the second issue of 2025. Thank you for your interest and support for our journal. In our journal, we strive to publish comprehensive and diverse articles in the field of Basic Sciences (Physics, Chemistry, Biology, and Mathematics). In this issue, we take pride in sharing a total of 5 articles, including 4 research papers, with our esteemed readers, contributing to the world of science. We wish all our readers enjoyable and productive reading.
Regards,

Prof. Dr. Dursun Ali KÖSE
On behalf of the HJS Editorial Board

INDEX

HİTİT JOURNAL OF SCIENCE

e-ISSN: 3061-9629
Volume: 2 • Number: 2
July 2025

Feeding Ecology of the Tawny Owl (*Strix aluco*) Population in Soğuksu National Park (Kızılcahamam-Ankara, Türkiye)

Şafak Bulut[1,*] | Burak Akbaba[2] | Zafer Ayaş[2]

[1]Gazi University, Faculty of Science, Department of Biology, Ankara, Türkiye.
[2]Hacettepe University, Faculty of Science, Department of Biology, Ankara, Türkiye.

Corresponding Author

Şafak BULUT
E-mail: safakbulut@gazi.edu.t
RORID[1]: ror.org/054xkpr46 RORID[2]: ror.org/04kwvgz42

Article Information

Article Type: Research Article
Doi: -
Received: 05.07.2025
Accepted: 16.07.2025
Published: 31.07.2025

Cite As

Bulut Ş., Akbaba B., Ayaş Z. Feeding Ecology of the Tawny Owl (*Strix aluco*) Population in Soğuksu National Park (Kızılcahamam-Ankara, Türkiye). Hitit journal of Science. 2025;2(2):26-30.

Peer Review: Evaluated by independent reviewers working in at least two different institutions appointed by the field editor.
Ethical Statement: Not available.
Plagiarism Checks: Yes - iThenticate
Conflict of Interest: The authors declare that they have no conflict of interest.
Acknowledgements: The authors would like to thank the management of Soğuksu National Park for access permission and field logistics. We also acknowledge the contributions of the laboratory assistants who supported the pellet dissection and prey identification process.
This study is part of the PhD dissertation of Şafak Bulut conducted at Hacettepe University.

CRedit Author Statement
Şafak Bulut: Conceptualization, Methodology, Investigation, Writing – Original Draft.
Burak Akbaba: Fieldwork Supervision, Validation, Resources, Visualization.
Zafer Ayaş: Project Administration, Writing – Review & Editing, Supervision.

(Roles assigned according to the CRediT taxonomy: https://credit.niso.org)

Feeding Ecology of the Tawny Owl (*Strix aluco*) Population in Soğuksu National Park (Kızılcahamam-Ankara, Türkiye)

Şafak Bulut1,* | Burak Akbaba2 | Zafer Ayaş2
[1]Gazi University, Faculty of Science, Department of Biology, Ankara, Türkiye.
[2]Hacettepe University, Faculty of Science, Department of Biology, Ankara, Türkiye.

Abstract
This study aims to investigate the feeding ecology of the Tawny Owl (*Strix aluco*) population in Soğuksu National Park, located in Central Anatolia, Türkiye. A total of 423 pellet samples were collected in 2014 and analyzed to identify prey remains to species level. The results revealed a diet dominated by small mammals, particularly M*icrotus subterraneus* (29.1%) and *Myodes glareolus* (19.8%). Parallel small mammal trapping yielded 758 individuals and was used to assess prey availability. A moderate but non-significant correlation was found between the abundance of prey and their representation in the owl's diet (r = 0.2955), suggesting that factors beyond numerical abundance, such as accessibility and habitat structure, influence prey selection. The calculated Levin's index (6.87) indicates a moderate dietary breadth. These findings highlight the owl's flexible foraging strategy in mosaic forest-steppe landscapes and support its use as an ecological indicator species in protected areas such as Soğuksu National Park.

Keywords: Tawny Owl, *Strix aluco*, pellet analysis, feeding ecology, Soğuksu National Park, small mammals, raptor

INTRODUCTION
The feeding ecology of the Tawny Owl (*Strix aluco*) in Soğuksu National Park, located in Kızılcahamam, Ankara, Turkey, exhibits several noteworthy characteristics influenced by environmental, seasonal, and ecological factors. Tawny Owls are predominantly generalist predators, exhibiting a diverse diet that varies according to habitat types and prey availability (Romanowski & Żmihorski, 2009; Capizzi, 2000; Rajković et al., 2024). Across various European habitats, they have been observed to prey on a wide range of taxa, including rodents, insects, and occasionally birds, reflecting their adaptability and opportunistic foraging strategies (Żmihorski & Osojca, 2006; Yatsiuk & Filatova, 2017; Zawadzka & Zawadzki, 2007). In their natural environment, Tawny Owls prefer woodland areas with a well-developed understory that supports their primary hunting method—ambush from elevated perches (Fröhlich & Ciach, 2017; Šotnár et al., 2020). Their diet is often dominated by small mammals such as voles (*Myodes glareolus*) and mice (*Apodemus* spp.), which are frequently the most abundant prey types (Luka & Riegert, 2018; Yatsiuk & Filatova, 2017). Studies have shown that periods of high vole abundance correlate with increased reproductive success and overall fitness in Tawny Owls, highlighting the crucial link between prey density and owl population dynamics (Luka & Riegert, 2018; Zawadzka & Zawadzki, 2007).

In Turkey, and particularly in the Central Anatolian region, studies on *Strix aluco* have begun to emerge more recently, contributing valuable data on regional diet patterns and habitat preferences. In Belgrad Forest near Istanbul, Arslangündoğdu et al. (2013) reported that 93% of prey remains found in pellets consisted of small rodents, especially *Apodemus* and *Microtus* species, while only 7% consisted of birds, amphibians, and insects. Tawny Owls in this region showed strong preferences for mature deciduous forests near water bodies. Playback surveys in the same study revealed 93 individuals, including 34 pairs, providing early population insights for the species in Turkey. In Central Anatolia, Nedyalkov and Boev (2016) documented a broader dietary range for Tawny Owls in semi-arid, rocky habitats. Their analysis revealed that small mammals constituted 76.3% of the diet, including *Mesocricetus brandti*, *Meriones tristrami*, and *Microtus cf. levis*, while birds—such as *Porzana porzana* and *Rallus aquaticus*—comprised 23.7% of prey items. This diversity was quantified by a Levins' Index of 10.65, indicating high dietary plasticity.

Seasonality also plays a vital role in shaping the feeding behavior of *Strix aluco*. Owls adjust their hunting patterns based on fluctuations in prey availability throughout the year, relying more heavily on small mammals during winter months when other prey becomes scarce (Romanowski & Żmihorski, 2009; Żmihorski & Osojca, 2006). In anthropogenically influenced or fragmented habitats, they demonstrate flexibility by incorporating alternative prey species and adapting to new habitat conditions (Rajković et al., 2024; Santoro et al., 2012; Zawadzka & Zawadzki, 2007). Environmental parameters such as elevation, climate, and habitat fragmentation further influence the species' foraging strategy. In Mediterranean and continental Anatolian regions, studies suggest that extreme temperatures and habitat heterogeneity may shape owl diet composition (Comay et al., 2022).

In this study, we investigated the feeding ecology of the Tawny Owl (*Strix aluco*) population in Soğuksu National Park, located in the Central Anatolian montane forest-steppe transition zone. We analyzed diet composition based on pellet contents, assessed prey availability through live trapping, and quantified dietary breadth using standardized indices to determine whether the population exhibits specialist or generalist foraging behavior.

MATERIALS AND METHODS
Study Area
The study was conducted in Soğuksu National Park (39°49'N, 32°38'E), located near Kızılcahamam in the Ankara province of Turkey. The park lies in the Central Anatolian biogeographic region and covers approximately 1,188 hectares. Elevation ranges from 1,050 to 1,750 meters above sea level. The dominant vegetation types include mixed coniferous and deciduous forest patches composed primarily of *Pinus nigra*, *Quercus* spp., and *Juniperus* spp., interspersed with open rocky habitats and grasslands. The climate is continental, characterized by hot, dry summers and cold, snowy winters.

Soğuksu National Park is part of the Important Bird Area (IBA) network and holds ecological significance due to its avian diversity and its role as a refuge for various raptor species.

Pellet Collection and Analysis

Pellet samples were collected between May and September 2014 from known roosting and nesting sites of Tawny Owls (*Strix aluco*) within the park boundaries. A total of 423 pellets were gathered non-invasively from beneath perches, tree cavities, and rocky ledges. The pellets were air-dried, measured, and dissected manually using forceps and a binocular stereomicroscope.

Prey remains were identified based on diagnostic features such as skulls, mandibles, and teeth, using reference collections and identification keys (e.g., Kryštufek & Vohralik, 2005; Niethammer, 1989). Prey items were grouped into major taxonomic categories: Rodentia, Insectivora, Aves, Amphibia, and Insecta.

Relative frequency (%) of prey types was calculated based on the number of individuals identified per taxonomic group. Bones found in multiple pellets were only counted once per pellet to avoid pseudoreplication.

Small Mammal Trapping

To assess the availability and diversity of small mammal species in the area, live trapping was conducted using Sherman traps in parallel with the pellet collection. Trapping was performed over 15 nights, covering different microhabitats (forest edge, steppe, and rocky zones). Traps were baited with apple slices and checked each morning. Captured individuals were identified, and released at the point of capture.

To assess the availability and diversity of small mammal species in the area, live trapping was conducted across five different habitat types between May and November in 2014 and 2015. Individuals were classified to species level, sexed, and weighed using standard procedures. Small mammal trapping was conducted monthly from May to November in 2014 and 2015, each sampling month comprising three consecutive nights. The total trapping effort amounted to 5250 trap-nights across five habitat types, with 1250 trap-nights conducted annually. These efforts complied with the ethical approval granted by the Hacettepe University Animal Research Ethics Committee (decision date: March 26, 2014; ref: 52338575-41).

Statistical Analysis

The correlation between prey abundance (from live trapping) and prey representation in pellets was evaluated using Pearson's correlation coefficient (r). Dietary breadth was calculated using Levins' index (B), and niche overlap between trapping and pellet data was measured with Pianka's index. Trophic niche breadth was calculated using Levins' index (1968), defined as $B=1/\sum p_i^2$, where p_i represents the proportion of each prey type in the diet. Standardized Levins' index (Hurlbert, 1978) was also computed to allow comparisons across studies with different prey category numbers. All statistical analyses were conducted in SPSS 20.0, with significance set at $p < 0.05$.

Results

Pellet Composition

A total of 423 regurgitated pellets from Tawny Owls (*Strix aluco*) were collected and analyzed. All pellets contained identifiable prey remains, yielding a total of 1,029 individual prey items assigned to five major taxonomic groups. The overall dietary composition was strongly dominated by small mammals, particularly rodents.

Rodentia constituted the majority of the diet (approximately 78.3%), with *Microtus subterraneus* (29.1%) and *Myodes glareolus* (19.8%) being the most frequent prey species. Murid rodents such as *Apodemus flavicollis* and Mus spp. were also frequently consumed. Insectivores (e.g., *Crocidura* spp.) accounted for 2.6% of prey items, while non-mammalian taxa—comprising birds, amphibians, and insects—collectively represented 19.2% of the diet When all major prey groups (including birds, amphibians, and insects) are included in the dietary analysis, the standardized Levin's index was recalculated as Ba = 0.53, indicating a moderate trophic niche breadth for the Tawny Owl population in Soğuksu National Park.

These results are summarized in Table 1, while the relative proportions of the five major prey groups are illustrated in Figure 1.

Table 1. Prey composition of Tawny Owl (*Strix aluco*) in Soğuksu National Park based on pellet analysis (n = 423). Frequencies are expressed as percentages of total identified prey items.

Prey Taxon	Frequency (%)
Microtus subterraneus	29.1
Myodes glareolus	19.8
Apodemus flavicollis	11.4
Mus spp.	6.1
Microtus spp. (undiff.)	4.8
Apodemus spp. (undiff.)	4.2
Crocidura spp.	2.6
Nannospalax xanthodon	1.3
Dryomys nitedula	0.8
Birds	8.2
Amphibians	6.1
Insects	3.3

Small Mammal Abundance

Live trapping efforts yielded 758 individuals from six small mammal species. The most commonly captured taxa were *Apodemus* spp. (54.9%), *Mus macedonicus* (15.2%), and *Myodes glareolus* (12.8%). *Microtus subterraneus* was captured at lower frequencies (11.6%) despite its high representation in the pellet data (Figure 2).

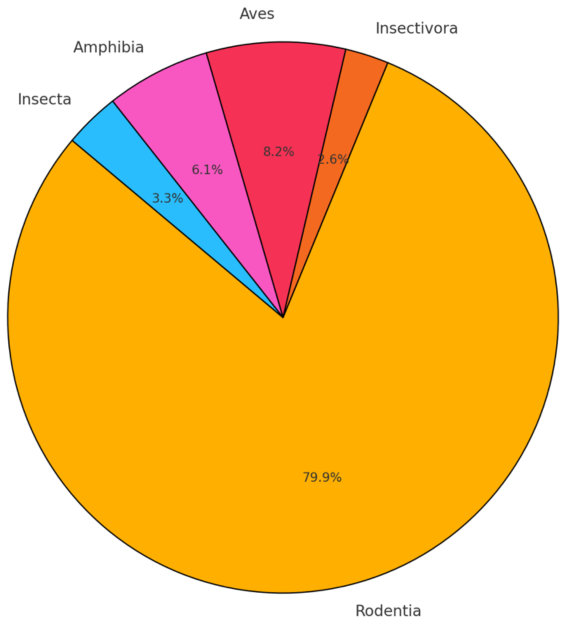

Figure 1. Relative proportions of major prey groups (Rodentia, Insectivora, Aves, Amphibia, Insecta) identified in Tawny Owl (Strix aluco) pellets collected from Soğuksu National Park.

Comparison of Diet and Prey Availability
To assess the relationship between prey availability and dietary composition, small mammal live trapping was conducted concurrently with pellet collection. A total of 758 individuals were captured, with *Apodemus* spp. being the most abundant (54.9%), followed by *Mus macedonicus* (15.2%), *Myodes glareolus* (12.8%), and *Microtus subterraneus* (11.6%). Other captured taxa included *Crocidura suaveolens* and *Dryomys nitedula*, albeit in lower frequencies.

When these trapping results were compared to pellet contents, several discrepancies were observed. Notably, Microtus subterraneus, although less frequently trapped, was disproportionately represented in the diet (29.1%). Conversely, Apodemus spp., the most abundant in the environment, were relatively underrepresented in the owl's diet (15.6%). This suggests that factors beyond abundance—such as detectability, habitat openness, and prey vulnerability—may influence prey selection.

A weak and statistically non-significant correlation was found between prey abundance in the environment and its representation in the owl's diet (Pearson's $r = 0.2955$, $p = 0.11$). Although not statistically significant, the trend suggests a weak tendency toward dietary selection aligned with availability.

A visual comparison of small mammal proportions from live trapping and pellet analysis is provided in Figure 2.

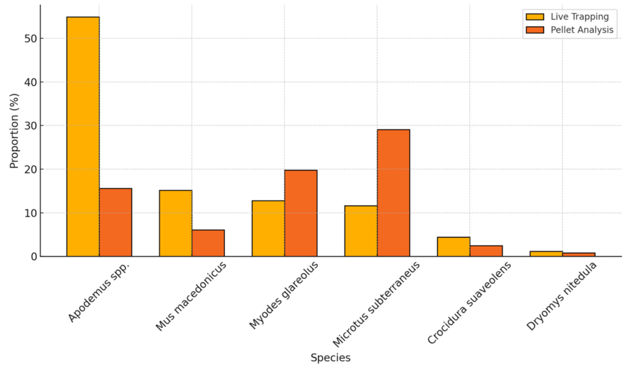

Figure 2. Comparison of small mammal species proportions based on live trapping and pellet analysis. Note the overrepresentation of *Microtus subterraneus* and underrepresentation of Apodemus spp. in the owl's diet relative to field availability.

Discussion

The feeding ecology of the Tawny Owl (*Strix aluco*) population in Soğuksu National Park reflects a combination of opportunistic foraging and context-dependent selectivity shaped by prey accessibility and habitat structure. Similar to findings across temperate European habitats, small mammals—particularly voles (*Microtus subterraneus*) and bank voles (*Myodes glareolus*)—comprised nearly half of the prey identified in owl pellets, confirming their role as staple prey in forested ecosystems (Romanowski & Żmihorski, 2009; Luka & Riegert, 2018; Zawadzka & Zawadzki, 2007).

Despite the high trapping frequency of *Apodemus* species (54.9%), their relative contribution to the diet was considerably lower (15.6%). This disparity suggests selective foraging, possibly due to microhabitat differences, prey detectability, or energetic profitability. Microtus species are typically more exposed in open or semi-open habitats, increasing their vulnerability during nocturnal ambush hunting from elevated perches (Šotnár et al., 2020). Similar mismatches between prey availability and consumption have been observed in Central and Eastern Europe, where foraging efficiency and prey accessibility, rather than sheer abundance, better explained dietary patterns (Fröhlich & Ciach, 2017).

Compared to other Turkish populations, the diet composition in Soğuksu is relatively consistent with findings from the Belgrad Forest in northwestern Turkey. There, Arslangündoğdu et al. (2013) found that 93% of prey items were rodents, predominantly *Apodemus* and *Microtus*, while only 7% were birds, amphibians, and insects. In contrast, our study revealed a more taxonomically diverse diet, with non-mammalian prey (birds, amphibians, insects) making up approximately 17.6% of total prey items. This difference may reflect ecological variation between deciduous lowland forests and the mixed montane habitats of Central Anatolia.

A broader prey spectrum was reported by Nedyalkov and Boev (2016) in the semi-arid regions of Central Anatolia, where the owl's diet included 12 mammal and 8 bird species, including wetland-associated taxa. Their calculated Levins'

Index of 10.65 suggested a high level of dietary plasticity. In comparison, the Levin's index calculated in our study (B = 6.87) and its standardized version (Ba = 0.53) indicate moderate trophic niche breadth, consistent with a generalist foraging strategy. The use of a standardized index allows meaningful comparisons across studies with differing prey category richness (Hurlbert, 1978), and in this case, supports the interpretation that S. aluco adjusts its diet based on local ecological constraints.

The weak but positive correlation between small mammal availability and diet composition ($r = 0.2955$, $p = 0.11$) further underscores the role of non-abundance factors in shaping foraging behavior. While not statistically significant, this trend suggests that habitat structure, prey detectability, and seasonal exposure may mediate prey selection. For instance, *Microtus subterraneus* may be more accessible during autumn due to decreased vegetation cover or reduced activity of diurnal predators (Petty, 1999; Sunde & Bolstad, 2004). The presence of generalist traits in the Tawny Owl should therefore be interpreted in light of such context-dependent ecological filters.

In summary, our findings confirm that the Tawny Owl in Soğuksu National Park exhibits a moderately broad trophic niche and displays flexible foraging behavior shaped by a combination of prey availability, habitat complexity, and seasonal patterns. The integration of pellet analysis with live-trapping data has provided a more nuanced understanding of diet composition and foraging selectivity, reinforcing the need for multi-method approaches in raptor feeding ecology studies.

Conclusion

This study provides the first comprehensive assessment of the feeding ecology of the Tawny Owl (*Strix aluco*) in Soğuksu National Park, Central Anatolia. Through pellet analysis and parallel small mammal trapping, we confirmed that the species displays a generalist but prey-selective feeding strategy, with a diet primarily composed of small rodents—particularly *Microtus subterraneus* and *Myodes glareolus*.

Despite Apodemus spp. being the most abundant in the environment, their relatively low representation in pellets suggests that prey behavior, habitat structure, and predator-prey interaction dynamics significantly influence prey choice. These results align with earlier findings from other Turkish regions (e.g., Istanbul and Karaman), yet they also emphasize the site-specific nature of owl foraging patterns.

The moderate dietary breadth observed (Levin's index = 6.87) indicates that Tawny Owls in this montane forest ecosystem rely on a stable core of prey species but may diversify when necessary. The species' capacity to adapt to different ecological contexts reinforces its role as a key indicator of ecosystem health and biodiversity.

From a conservation standpoint, maintaining heterogeneous landscapes that support diverse small mammal populations—particularly in forest–steppe mosaics—is crucial. Long-term monitoring of apex predators like *Strix aluco* can serve as an effective tool for evaluating habitat quality and guiding forest and wildlife management strategies in protected areas such as Soğuksu National Park.

References

1. Arslangündoğdu Z, Beşkardeş V, Smith LD, Yüksel U. The Tawny Owl (*Strix aluco* L., 1758) population in Belgrad Forest, Istanbul – Turkey. *J Fac For Istanbul Univ*. 2013;63(1):11–17.
2. Capizzi D. Diet shifts of the Tawny Owl *Strix aluco* in central and northern Italy. *Ital J Zool*. 2000;67(1):73–79. https://doi.org/10.1080/11250000009356298
3. Comay O, Ezov E, Yom-Tov Y, Dayan T. In its southern edge of distribution, the Tawny Owl (*Strix aluco*) is more sensitive to extreme temperatures than to rural development. *Animals*. 2022;12(5):641. https://doi.org/10.3390/ani12050641
4. Fröhlich A, Ciach M. Noise pollution and decreased size of wooded areas reduce the probability of occurrence of Tawny Owl *Strix aluco*. *Ibis*. 2017;160(3):634–646. https://doi.org/10.1111/ibi.12554
5. Hurlbert SH. (1978). The measurement of niche overlap and some relatives. *Ecology*, 59(1), 67–77.
6. Levins R. (1968). *Evolution in changing environments*. Princeton University Press.
7. Luka V, Riegert J. *Apodemus* mice as the main prey that determines reproductive output of Tawny Owl (*Strix aluco*) in Central Europe. *Popul Ecol*. 2018;60(3):237–249. https://doi.org/10.1007/s10144-018-0611-z
8. Nedyalkov N, Boev Z. Diet of Barn Owl *Tyto alba* and Tawny Owl *Strix aluco* in Central Anatolia, Turkey. *Sandgrouse*. 2016;38(1):79–81.
9. Pagaldai N, Arizaga J, Jiménez-Franco M, Zuberogoitia Í. Colonization of urban habitats: Tawny Owl abundance is conditioned by urbanization structure. *Animals*. 2021;11(10):2954. https://doi.org/10.3390/ani11102954
10. Rajković D, Stanković D, Šeat J, Stevanović D, Stošović M, Skorić S. Spatial ecology of a resident avian predator during the non-breeding period in managed habitats of southeastern Europe. *Animals*. 2024;14(22):3338. https://doi.org/10.3390/ani14223338
11. Romanowski J, Żmihorski M. Seasonal and habitat variation in the diet of the Tawny Owl (*Strix aluco*) in Central Poland during unusually warm years. *Biologia*. 2009;64(2):365–369. https://doi.org/10.2478/s11756-009-0036-4
12. Santoro M, Mattiucci S, Nascetti G, Kinsella J, Prisco F, Troisi S, et al. Helminth communities of owls (Strigiformes) indicate strong biological and ecological differences from birds of prey in southern Italy. *PLoS ONE*. 2012;7(12):e53375. https://doi.org/10.1371/journal.pone.0053375
13. Šotnár K, Obuch J, Pačenovský S, Jarčuška B. Spatial distribution of four sympatric owl species in Carpathian montane forests. *Raptor J*. 2020;14(1):1–13. https://doi.org/10.2478/srj-2020-0002
14. Yatsiuk Y, Filatova Y. Seasonal changes in Tawny Owl (*Strix aluco*) diet in an oak forest in Eastern Ukraine. *Turk J Zool*. 2017;41:130–137. https://doi.org/10.3906/zoo-1509-43
15. Zawadzka D, Zawadzki J. Feeding ecology of Tawny Owl (*Strix aluco*) in Wigry National Park (Northeast Poland). *Acta Zool Lit*. 2007;17(3):234–241. https://doi.org/10.1080/13921657.2007.10512837
16. Żmihorski M, Osojca G. Diet of the Tawny Owl (*Strix aluco*) in the Romincka Forest (Northeast Poland). *Acta Zool Lit*. 2006;16(1):54–60. https://doi.org/10.1080/13921657.2006.10512710
17. Zuberogoitia Í, Burgos G, González-Oreja JA, Morant J, Martínez JE, Zabala J. Factors affecting spontaneous vocal activity of Tawny Owls *Strix aluco* and implications for surveying large areas. *Ibis*. 2018;161(3):495–503. https://doi.org/10.1111/ibi.12684

HİTİT JOURNAL OF SCIENCE

e-ISSN: 3061-9629
Volume: 2 • Number: 2
July 2025

Existence and approximation for nonlinear dynamic equations using monotone iteration method

Nour H. M. Alsharif

Department of Mathematics, Graduate School of Natural and Applied Sciences, Dokuz Eylül University, Izmir, Türkiye.

Corresponding Author

Nour H. M. Alsharif
E-mail: nhmalsharif@gmail.com
RORID: ror.org/00dbd8b73

Article Information

Article Type: Research Article
Doi: -
Received: 15.04.2025
Accepted: 02.06.2025
Published: 31.07.2025

Cite As

Alsharif NHM.. Existence and approximation for nonlinear dynamic equations using monotone iteration method. Hitit journal of Science. 2025;2(2):31-36.

Peer Review: Evaluated by independent reviewers working in at least two different institutions appointed by the field editor.
Ethical Statement: Not available.
Plagiarism Checks: Yes - iThenticate
Conflict of Interest: Author approves that to the best of their knowledge, there is not any conflict of interest or common interest with an institution/organization or a person that may affect the review process of the paper.
Acknowledgements: The author received no financial support for the research, authorship, and/or publication of this article.

CRedit Author Statement
Nour H. M. Alsharif: Design of the study, Conceptualization, Writing-original draft, Editing, Supervision.

Existence and approximation for nonlinear dynamic equations using monotone iteration method

Nour H. M. Alsharif
Department of Mathematics, Graduate School of Natural and Applied Sciences, Dokuz Eylül University, Izmir, Türkiye.

Abstract

This paper improves a generalized monotone iterative technique for solving dynamic initial value problems (IVPs) on time scales, using the method of coupled lower and upper solutions. We construct monotone sequences of iterates, each of which corresponds to a solution of the dynamic IVP on time scales. Under suitable conditions, we establish the uniform and monotonic convergence of sequences to the extremal (minimal and maximal) solutions of the problem. The results provide a unified framework for analyzing dynamic equations on time scales via monotone iteration.

Keywords: Comparison result, Monotone iterative technique, Coupled upper and lower solutions

INTRODUCTION

In recent decades, the theory of dynamic equations on time scales has played a pivotal role in unifying and extending the frameworks of differential and difference equations [2,4].

The monotone iterative technique, coupled with the method of lower and upper solutions, has proven to be a powerful and flexible tool for establishing existence results for nonlinear differential equations [3,5,6,7]. In 2002 and 2004, Bhaskar [1] and West [10] advanced this methodology by developing a generalized monotone iterative technique for initial value problems (IVPs). Their work demonstrated the existence of minimal and maximal solutions for differential equations where the nonlinear function decomposes into the sum of a monotone non-decreasing and a monotone non-increasing function. At this stage, Ramirez and Vatsala [8] extended these results to Caputo fractional differential equations with periodic boundary conditions via an initial value problem approach. Meanwhile, Wang and Tian [9] introduced an alternative method to derive unique solutions for boundary value problems.

In this study, we employ the method of coupled lower and upper solutions for dynamic initial value problems on a time scale $\mathbb{T}$ By constructing monotone iterative sequences from corresponding linear IVPs, we establish the uniform and monotone convergence of these sequences to the coupled minimal and maximal solutions of the nonlinear dynamic IVP.

Our results hold under the assumption that the nonlinear function f is rd-continuous and can be expressed as the difference of two monotone non-decreasing functions.

The paper is organized as follows. In Section 2, we review some basic concepts and preliminary results. The main results are presented in Section 3 followed by their proofs in Section 4. In Section 5 we present numerical examples to motivate the applicability and relevance of the main results. Concluding remarks are provided in Section 6.

PRELIMINARIES

In this section, we mention some basic concepts and theories used in subsequent references.

A time scale $\mathbb{T}$ is any nonempty closed subset of $\mathbb{R}$. The intervals with a subscript $\mathbb{T}$ are used to indicate the ordinary interval intersects with $\mathbb{T}$, i.e., $[a,b]_{\mathbb{T}} = [a,b] \cap \mathbb{T}$. The forward jump operator $\sigma : \mathbb{T} \to \mathbb{T}$ and backward jump operator $\rho : \mathbb{T} \to \mathbb{T}$ are defined respectively by

$$\sigma(t) = \inf\{s > t : s \in \mathbb{T}\} \text{ and } \rho(t) = \sup\{s < t : s \in \mathbb{T}\}$$

A point is called right-scattered, right-dense, left-scattered and left-dense if $\sigma(t) > t, \sigma(t) = t, \rho(t) < t$ and $\rho(t) = t$; respectively. Points that are both right- and left-scattered are isolated, while those that are both right- and left-dense are dense. The graininess function $\mu^* : \mathbb{T} \to [0,\infty)$is given by $\mu^*(t) = \sigma(t) - t$. The mapping $f : \mathbb{T} \to \mathbb{R}^n$ is said to be differentiable, if f has exactly one derivative $f^{\Delta}(t)$; that is, given any $\varepsilon > 0$, there exists a neighborhood U_t of t such that f satisfies

$$\left|f(\sigma(t)) - f(s) - f^{\Delta}(t)\,(\sigma(t) - s)\right| \le \varepsilon\,|\sigma(t) - s| \text{ for } s \in U_t$$

The set $\mathbb{T}^{\kappa}$ is defined as

$$\mathbb{T}^{\kappa} := \begin{cases} \mathbb{T} \setminus (\rho(\mathbb{T}), \sup \mathbb{T}], & \text{if } \sup \mathbb{T} < \infty; \\ \mathbb{T}, & \text{if } \sup \mathbb{T} = \infty. \end{cases}$$

A function $f : \mathbb{T} \to \mathbb{R}$ is regulated if it has finite left-sided limits at left-dense points. A function $f : \mathbb{T} \times \mathbb{R}^n \to \mathbb{R}^n$ is rd-continuous (denoted $f \in \mathscr{C}_{\mathrm{rd}}[\mathbb{T} \times \mathbb{R}^n, \mathbb{R}^n]$if it is continuous at each right-dense $t \in \mathbb{T}$, and the left sided limit $f(t^-, x)$ exists in each left-dense. A function $F : \mathbb{T}^{\kappa} \to \mathbb{R}$ is an antiderivative of $f : \mathbb{T}^{\kappa} \to \mathbb{R}$ if $F^{\Delta}(t) = f(t)$ for all $t \in \mathbb{T}^{\kappa}$. In this case, the delta integral of f is $\int_a^t f(s)\Delta s = F(t) - F(a)$, $t \in \mathbb{T}$.

Consider the dynamic initial value problem (IVP)

$$u^{\Delta} = f(t,u) \text{ for } t \in [t_0, \infty)_{\mathbb{T}} \tag{1}$$

with $u(t_0) = u_0$ As usual here the time scale $\mathbb{T}$ is assumed to have $t = t_0$ as the minimal element and $t = \tilde{t}$ as the maximal element which is not left scattered.

We need the following definitions before we proceed further.

Definition 1. A function $f : \mathscr{C}[\mathbb{T} \times \mathbb{R}^n, \mathbb{R}^n]$ is quasi-monotone non-decreasing if $x \le y$ and $x_i = y_i$ for some $i \in \mathbb{N}$ implies $f_i(t,x) \le f_i(t,y)$.

Definition 2. A function $u \in \mathscr{C}[[t_0,\infty)_{\mathbb{T}}, \mathbb{R}^n]$ is a solution of (1) for some $s \in [t_0,\infty)_{\mathbb{T}}$ if it differentiable on $[s,\infty)_{\mathbb{T}}$ and satisfies (1) identically on $[s,\infty)_{\mathbb{T}}$ with $u(t_0) = u_0$.

Now, let us introduce comparison theorem.

Theorem 1 ([4]). Let $\mathbb{T}$ be a time scale with $t_0 \ge 0$ as its minimal element (no maximal element). Suppose

(i) $v, w \in \mathscr{C}\mathrm{rd}^1[\mathbb{T}, \mathbb{R}^n]$ for each $t \in \mathbb{T}$ and satisfy the following inequalities

$$v^{\Delta}(t) \le f(t, v(t)), \quad v(t_0) \le u_0$$
$$w^{\Delta}(t) \ge f(t, w(t)), \quad w(t_0) \ge u_0 \tag{2}$$

(ii) $f \in \mathscr{C}_{\mathrm{rd}}[\mathbb{T} \times \mathbb{R}^n, \mathbb{R}^n]$, $f(t,u)$ is quasi-monotone non-decreasing in u and for each $i \in \mathbb{N}$, $1 \le i \le n$, $f_i(t,u)\mu^*(t) + u_i$, is non-decreasing in u_i for $t \in \mathbb{T}$.

Moreover, let $f(t,u)$ satisfies the following condition

$$f_i(t,x) - f_i(t,y) \le L \sum_{i=1}^{n} (x_i - y_i) \text{ for } x \ge y, L > 0. \tag{3}$$

Then $v(t_0) \le w(t_0)$ implies that $v(t) \le w(t)$ for $t \in \mathbb{T}$.

We conclude the following corollaries which will be useful in our main results.

Corollary 1. If $g \in \mathscr{C}_{\mathrm{rd}}{}^1[\mathbb{T}, \mathbb{R}^n]$ satisfies $g^{\Delta}(t) \le 0$ and $g(t_0) \le 0$, then $g(t) \le 0$ for all $t \in \mathbb{T}$.
Corollary 2. If $g \in \mathscr{C}_{\mathrm{rd}}{}^1[\mathbb{T}, \mathbb{R}^n]$ satisfies $g^{\Delta}(t) \ge 0$ and $g(t_0) \ge 0$, then $g(t) \ge 0$ for all $t \in \mathbb{T}$.

Now, consider the nonlinear dynamic initial value problem

$$u^{\Delta}(t) = f_1(t, u(t)) - f_2(t, u(t)), \quad u(0) = u_0, \tag{4}$$

where $f_1(t,u)$ and $f_2(t,u)$ may be non-decreasing functions.

Firstly, we introduce four types of coupled lower and upper solutions for (4).

Definition 3. Let $v_0, w_0 \in \mathscr{C}_{\mathrm{rd}}{}^1[\mathbb{T}, \mathbb{R}]$. Then v_0, w_0 are said to be for all $t \in \mathbb{T}$.

(i) natural lower and upper solutions of (4), if

$$v_0{}^{\Delta}(t) \le f_1(t, v_0(t)) - f_2(t, v_0(t)),\ v_0(0) \le u_0$$
$$w_0{}^{\Delta}(t) \ge f_1(t, w_0(t)) - f_2(t, w_0(t)),\ w_0(0) \ge u_0$$

(ii) coupled lower and upper solutions of Type I of (4), if

$$v_0{}^{\Delta}(t) \le f_1(t, v_0(t)) - f_2(t, w_0(t)),\ v_0(0) \le u_0$$
$$w_0{}^{\Delta}(t) \ge f_1(t, w_0(t)) - f_2(t, v_0(t)),\ w_0(0) \ge u_0$$

(iii) coupled lower and upper solutions of Type II of (4), if

$$v_0{}^{\Delta}(t) \le f_1(t, w_0(t)) - f_2(t, v_0(t)),\ v_0(0) \le u_0$$
$$w_0{}^{\Delta}(t) \ge f_1(t, v_0(t)) - f_2(t, w_0(t)),\ w_0(0) \ge u_0$$

(iv) coupled lower and upper solutions of Type III of (4) if

$$v_0{}^{\Delta}(t) \le f_1(t,,, w_0(t)) - f_2(t,,, w_0(t)), \quad v_0(0) \le u_0$$
$$w_0{}^{\Delta}(t) \ge f_1(t,,, v_0(t)) - f_2(t,,, v_0(t)), \quad w_0(0) \ge u_0$$

MAIN RESULTS

In this section, we now present our main results on the existence and convergence of solutions to the nonlinear dynamic equation (4). Our approach leverages coupled lower and upper solutions to construct monotone iterative sequences that converge uniformly to extremal solutions. Theorem 2 employs Type I coupled solutions, we derive natural monotone sequences that converge uniformly and monotonically to the coupled minimal and maximal solutions of Type I of (4). We can also give result using coupled lower and upper solutions of Type I and Type III, however it require an additional assumption to obtain intertwined monotone sequences which converge uniformly to coupled minimal and maximal solutions of (4).

Theorem 2. Assume the following conditions hold
(A1) the functions v_0, w_0 are coupled lower and upper solutions of Type I for (4) satisfying $v_0(t) \le u \le w_0(t)$ for all $t \in \mathbb{T}$,
(A2) the functions $f_1, f_2 \in C^{\mathrm{rd}}(\mathbb{T}^{\kappa} \times \mathbb{R}^n, \mathbb{R}^n)$, $f_1(t,u)$ and $f_2(t,u)$ are non-decreasing in u for each $t \in \mathbb{T}$.

Then, there exist monotone sequences $(v_j(t))$ and $(w_j(t))$ generated by the iterative scheme such that $v_j(t) \to \alpha(t)$ and $w_j(t) \to \beta(t)$ are uniformly convergent and monotonically, where α, β are coupled minimal and maximal solutions of (4), respectively. Moreover, they satisfy the coupled system

$$\alpha^{\Delta} = f_1(t,\alpha) - f_2(t,\beta), \quad \alpha(0) = u_0$$
$$\beta^{\Delta} = f_1(t,\beta) - f_2(t,\alpha), \quad \beta(0) = u_0$$

for all $t \in \mathbb{T}$.

Theorem 3. Assume conditions (A1) and (A2) of Theorem 2 hold. Consider the iterative scheme

$$v_{j+1}{}^{\Delta} = f_1(t, w_j) - f_2(t, v_j), \quad v_{j+1}(0) = u_0 = w_j(t_0),$$
$$w_{j+1}{}^{\Delta} = f_1(t, v_j) - f_2(t, w_j), \quad w_{j+1}(0) = u_0 = v_j(t_0). \tag{5}$$

Then, the iterates generate monotone sequences $\{v_{2j}\}$, $\{v_{2j+1}\}$, $\{w_{2j}\}$ and $\{w_{2j+1}\}$ satisfying

$$v_0 \le w_1 \le \ldots \le v_{2j} \le w_{2j+1} \le v_{2j+1} \le w_{2j} \le \ldots \le v_1 \le w_0$$

for all $j \in \mathbb{N}$ on $\mathbb{T}$, provided $v_0 \le u \le w_0$. Furthermore, the sequences converge $\{v_{2j}\}$ and $\{w_{2j+1}\}$ converge uniformly to α, and $\{v_{2j+1}\}$ and $\{w_{2j}\}$ converge uniformly to β, where α and β are coupled minimal and maximal solutions of Type I, respectively, of the system

$$\alpha^{\Delta} = f_1(t,\alpha) - f_2(t,\beta), \quad \alpha(0) = u_0$$
$$\beta^{\Delta} = f_1(t,\beta) - f_2(t,\alpha), \quad \beta(0) = u_0 \tag{6}$$

PROOF OF THE MAIN RESULTS

Here, we present proof of the our main results.
Proof of Theorem 2. For each $j \ge 0$, consider the system

$$v_{j+1}{}^{\Delta} = f_1(t, v_m) - f_2(t, w_j), \quad v_{j+1}(0) = u_0,$$
$$w_{j+1}{}^{\Delta} = f_1(t, w_j) - f_2(t, v_j), \quad w_{j+1}(0) = u_0. \tag{7}$$

By assumption, $v_0(0) \le u_0 \le w_0(0)$. From (7), we have

$$v_1{}^{\Delta} = f_1(t, v_0) - f_2(t, w_0), \quad v_1(0) = u_0,$$
$$w_1{}^{\Delta} = f_1(t, w_0) - f_2(t, v_0), \quad w_1(0) = u_0.$$

We now show that $v_0 \le v_1 \le u \le w_1 \le w_0$ on $\mathbb{T}$. Let $\psi = w_1 - w_0$. Then, $\psi(0) \le 0$, and

$$\begin{aligned}\psi^{\Delta} &= w_1{}^{\Delta} - w_0{}^{\Delta} \\ &\le f_1(t, w_0) - f_2(t, v_0) - f_1(t, w_0) + f_2(t, v_0) \\ &= 0.\end{aligned}$$

By Corollary 1, $\psi(t) \le 0$, so $w_1(t) \le w_0(t)$ on $\mathbb{T}$. Similarly, we can show that $v_1 \ge v_0$ on $\mathbb{T}$. Next, let $\phi = u - w_1$. Since $\phi(0) = 0$ and

$$\begin{aligned}\phi^{\Delta} &= u^{\Delta} - {w_1}^{\Delta}\\ &= f_1(t,u) - f_2(t,u) - f_1(t,w_0) + f_2(t,v_0)\\ &\le 0\end{aligned}$$

it follows that $u(t) \le w_1(t)$ on $\mathbb{T}$. Similarly, $u(t) \ge v_1(t)$. Thus, $v_0 \le v_1 \le u \le w_1 \le w_0$ holds for $k = 1$. Assume by induction that for some $k > 1$,

$$v_{k-1} \le v_k \le u \le w_k \le w_{k-1} \tag{8}$$

holds on $\mathbb{T}$. We now prove

$$v_k \le v_{k+1} \le u \le w_{k+1} \le w_k \quad \text{on } \mathbb{T}. \tag{9}$$

Let $\psi = w_{k+1} - w_k$. Then, $\psi(0) = 0$ and

$$\begin{aligned}\psi^{\Delta} &= {w^{\Delta}}_{k+1} - {w^{\Delta}}_k\\ &= f\_1(t,w_k) - f\_2(t,v_k) - f\_1(t,w_{k-1}) + f\_2(t,v_{k-1})\\ &\le 0.\end{aligned}$$

Thus, $w_{k+1}(t) \le w_k(t)$. Similarly, $v_{k+1}(t) \ge v_k(t)$. Now, let $\varphi = u - w_{k+1}$. Since $\varphi(0) = 0$ and

$$\begin{aligned}\varphi^{\Delta} &= u^{\Delta} - {w^{\Delta}}_{k+1}\\ &= f_{\_1}(t,u) - f_{\_2}(t,u) - f_{\_1}(t,w_k) + f_{\_2}(t,v_k)\\ &\le 0,\end{aligned}$$

we have $u(t) \le w_{k+1}(t)$. Similarly, $u(t) \ge v_{k+1}(t)$. By induction, we conclude that

$$v_0 \le v_1 \le \ldots \le v_j \le u \le w_j \le \ldots \le w_1 \le w_0 \text{ on } \mathbb{T}. \tag{10}$$

To show uniform convergence of $\{v_j\}$ and $\{w_j\}$, we prove they are uniformly bounded and equicontinuous. From (10) both sequences are uniformly bounded. For equicontinuity, let $0 \le t_1 \le t_2$ on $\mathbb{T}$. For $j > 0$,

$$\begin{aligned}|w_j(t_1) - w_j(t_2)| &= \left|\int_{t_1}^{t_2} [f_1(s,w_{j-1}(s)) - f_2(s,v_{j-1}(s))\Delta s\right|\\ &\le \int_{t_2}^{t_1} |f_1(s,w_{j-1}(s)) - f_2(s,v_{j-1}(s))|\Delta s.\end{aligned}$$

Since $\{v_j\}$ and $\{w_j\}$ are uniformly bounded and f_1, f_2 are bounded on $\mathbb{T}$, there exists $\gamma > 0$ such that

$$|w_j(t_1) - w_j(t_2)| \le \gamma |t_1 - t_2|$$

Thus, for any $\varepsilon > 0$, choosing $\delta = \frac{\varepsilon}{\gamma}$ ensures $|w_j(t_1) - w_j(t_2)| \le \varepsilon$ whenever $|t_1 - t_2| \le \delta$ Similarly, $\{v_j\}$ is equicontinuous. By the Arzelà-Ascoli theorem, there exist subsequences $\{v_{j_k}\}$ and $\{w_{j_k}\}$ converging uniformly to $\alpha(t)$ and $\beta(t)$, respectively. The monotonicity of $\{v_j\}$ and $\{w_j\}$ implies uniform convergence of the entire sequences. To show that α and β are coupled solutions of Type I for (4), integrate (7)

$$\begin{aligned}v_{j+1}\left(t\right) &= u_0 + \int_0^t [f_1(s,v_j(s)) - f_2(s,w_j(s))]\Delta s\\ w_{j+1}\left(t\right) &= u_0 + \int_0^t [f_1(s,w_j(s)) - f_2(s,v_j\ (s))]\Delta s\end{aligned} \tag{11}$$

Taking $j \to \infty$ and using uniform convergence, we obtain

$$\begin{aligned}\alpha\left(t\right) &= u_0 + \int_0^t [f_1(s,\alpha(s)) - f_2(s,\beta(s))]\Delta s,\\ \beta\left(t\right) &= u_0 + \int_0^t [f_1(s,\beta(s)) - f_2(s,\alpha(s))]\Delta s.\end{aligned} \tag{12}$$

Differentiating yields

$$\begin{aligned}\alpha^{\Delta} &= f_1(t,\alpha) - f_2(t,\beta),\ \alpha(0) = u_0,\\ \beta^{\Delta} &= f_1(t,\beta) - f_2(t,\alpha),\ \beta(0) = u_0.\end{aligned}$$

Finally, since $v_0 \le v_j \le u \le w_j \le w_0$ for all j, taking $j \to \infty$ gives $v_0 \le \alpha \le u \le \beta \le w_0$ on $\mathbb{T}$. Thus, α and β are coupled minimal and maximal solutions of Type I for (4), respectively. This completes the proof.

Proof of Theorem 3. By assumption, $v_0 \le u \le w_0$ on . From the iterative scheme (5), we derive the first iterates

$$\begin{aligned}{v_1}^{\Delta} &= f_1(t,w_0) - f_2(t,v_0), \quad v_1(0) = u_0,\\ {w_1}^{\Delta} &= f_1(t,v_0) - f_2(t,w_0), \quad w_1(0) = u_0.\end{aligned}$$

We first show $w_1 \le w_0$ on $\mathbb{T}$. Let $\phi = w_1 - w_0$. Then $\phi(0) \le 0$ and

$$\begin{aligned}\phi^{\Delta} &= {w_1}^{\Delta} - {w_0}^{\Delta}\\ &\le f_1(t,v_0) - f_2(t,w_0) - f_1(t,w_0) + f_2(t,v_0)\\ &= (f_1(t,v_0) - f_1(t,w_0)) + (f_2(t,v_0) - f_2(t,w_0))\\ &\le 0,\end{aligned}$$

since \$$v_0 \le w_0$ and f_1, f_2 are nondecreasing. By Corollary 1, $\phi(t) \le 0$, proving $w_1 \le w_0$. Similarly, $v_0 \le v_1$. Next, we verify the ordering $v_0 \le w_1 \le v_1 \le w_0$. Let $\psi = v_1 - w_0$. Then, $\psi(0) \le 0$, and

$$\psi^{\Delta} \le f(t,,,w_0) - f(t,,,v_0) - f(t,,,w_0) + f(t,,,v_0) = 0$$

Thus, $v_1 \le w_0$. Let $\varphi = w_1 - v_1$. Then, $\varphi(0) = 0$, and

$$\varphi^{\Delta} = (f_1(t,v_0) - f_1(t,w_0)) + (f_2(t,v_0) - f_2(t,w_0)) \le 0$$

Hence, $w_1 \le v_1$. Assume for some $k \ge 1$,

$$v_{2k-2} \le w_{2k-1} \le v_{2k} \le w_{2k} \le v_{2k-1} \le w_{2k-2} \text{ on } \mathbb{T}.$$

We show the ordering extends to $k + 1$

$$v_{2k} \le w_{2k+1} \le v_{2k+2} \le w_{2k+2} \le v_{2k+1} \le w_{2k} \text{ on } \mathbb{T}.$$

Let $\psi = v_{2k} - w_{2k+1}$. Then,

$$\psi^{\Delta} \le f_1(t,w_{2k-1}) - f_1(t,v_{2k}) + f_2(t,w_{2k}) - f_2(t,v_{2k-1}) \le 0,$$

since $w_{2k-1} \le v_{2k}$ and $w_{2k} \le v_{2k-1}$.
Analogously, $\varphi = w_{2k+1} - v_{2k+1}$ yields $\varphi^{\Delta} \le 0$. By induction, we get

$$v_0 \le w_1 \le \cdots \le v_{2j} \le w_{2j+1} \le v_{2j+1} \le w_{2j} \le \cdots \le v_1 \le w_0 \text{ on } \mathbb{T}. \tag{13}$$

As in Theorem 2, the sequences $\{v_{2j}, w_{2j+1}\}$ and $\{v_{2j+1}, w_{2j}\}$ converge uniformly to α and β, respectively, satisfying the coupled system

$$\alpha^\Delta = f_1\left(t,\alpha\right) - f_2\left(t,\beta\right), \quad \alpha\left(0\right) = u_0,$$
$$\beta^\Delta = f_1\left(t,\beta\right) - f_2\left(t,\alpha\right), \quad \beta\left(0\right) = u_0.$$

For all j, $v_{2j} \le w_{2j+1} \le u \le v_{2j+1} \le w_{2j}$. Taking limits as $j \to \infty$, we obtain

$$v_0 \le \alpha \le u \le \beta \le w_0 \text{ on } \mathbb{T}.$$

proving α and β are coupled minimal and maximal solutions of Type I for (4).

ILLUSTRATIVE EXAMPLES

We give some examples which are application of Theorem 2 and Theorem 3.

Example 1.
Consider the nonlinear dynamic equation

$$u^\Delta(t) = \frac{u^2}{2}(t) - \frac{u}{4}(t) \quad \text{for} t \in (0,1)\mathbb{R} \tag{14}$$

with the initial condition $u(0) = -1$. Define the functions $v_0, w_0 : [0,1]_{\mathbb{R}} \to \mathbb{R}$ by

$$v_0(t) = -1 \quad \text{and} \quad w_0(t) = t-1 \quad \text{for all } t \in [0,1]_{\mathbb{R}}.$$

Observe that $v_0(t) \le w_0(t)$ for all $[0,1]_{\mathbb{R}}$, and $v_0(0) = w_0(0) = -1 = u(0)$.

We now verify that v_0 and w_0 are coupled lower and upper solutions of Type I for (14). Then,

$$v_0{}^\Delta(t) = 0 \le \frac{3}{4} - \frac{t}{4} \quad \text{for all} \quad t \in (0,1)_{\mathbb{R}}$$

and

$$w_0{}^\Delta(t) = 1 \ge \frac{(t-1)^2}{2} + \frac{1}{4} \quad \text{for all} \quad t \in (0,1)_{\mathbb{R}}$$

Thus, v_0, w_0 satisfy the conditions for coupled lower and upper solutions of Type I for (14). Furthermore, assumptions (A1) and (A2) are readily verified. By Theorem 2, there exist monotone sequences that converge uniformly to the extremal solutions of (14) in the sector $[-1, t-1]$, and, by Theorem 3, alternating sequences also converge to the extremal solutions.

Example 2.
Let $\mathbb{T} = \mathbb{N}_0 = \{0,1,2,\ldots\}$, and consider the nonlinear dynamic equation

$$u^\Delta(t) = u(t) + t - te^{-u(t)} \quad \text{for} \quad t \in [0,,,\infty)_{\mathbb{T}} \tag{15}$$

with the initial condition $u(0) = 1$. Define the functions $v_0, w_0 : \mathbb{T} \to \mathbb{R}$ by

$$v_0(t) = 0 \quad \text{and} \quad w_0(t) = 2^t \quad \text{for all} \quad t \in \mathbb{T}.$$

Obviously, $v_0(t) \le w_0(t)$ for $t \in \mathbb{T}$. Moreover, we verify that v_0 and w_0 are coupled lower and upper solutions of Type I for (15). Indeed,

$$v_0{}^\Delta(t) = 0 \le t\left(1 - e^{-2^t}\right) \quad \text{for all} \quad t \in \mathbb{T}$$

and

$$w_0{}^\Delta(t) = 2^t \ge 2^t \quad \text{for all} \quad t \in \mathbb{T}$$

It is straightforward to check those conditions (A1) and (A2) are satisfied. By Theorem 2, we conclude the existence of monotone sequences that converge uniformly to the extremal solutions of (15) within the sector $\left[0, 2^t\right]$. Additionally, by Theorem 3, there exist alternating sequences that also converge to extremal solutions.

CONCLUSION

In this work, we have developed a comprehensive monotone iterative method for dynamic equations with initial value problems on time scales. Our approach, based on the fundamental concepts of coupled lower and upper solutions, successfully constructs natural and intertwined monotone sequences that converge uniformly to coupled extremal solutions. We make our final comments to conclude the paper.

Corollary 3. In addition to assumption of the Theorem 2, if for $u_1 \ge u_2$ and f_1, f_2 satisfy

$$\begin{aligned} f_1(t,u_1) - f_1(t,u_2) \le L_1(u_1 - u_2), \\ f_2(t,u_1) - f_2(t,u_2) \le L_2(u_1 - u_2), \end{aligned} \tag{14}$$

where L_1, L_2>0. Then $\alpha(t) = u(t) = \beta(t)$ is the unique solution.
Proof. We know that ; and so, we need to prove that . Let $p(t) = \beta(t) - \alpha(t)$ then $p(0) = 0$ and by using (14), it follows that

$$\begin{aligned} & p^\Delta\left(t\right) = \beta^\Delta\left(t\right) - \alpha^\Delta\left(t\right) \\ & = f_1(t,\beta(t)) - f_2(t,\alpha(t)) - f_1(t,\alpha(t)) + f_2(t,\beta(t)) \\ & \le L_1(\beta(t) - \alpha(t)) + L_2(\beta(t) - \alpha(t)) \\ & \le (L_1 + L_2)p(t) \end{aligned}$$

Thus, we get by Theorem 1 that $p(t) \le 0$, which proves that $\beta(t) \le \alpha(t)$ Hence, $\alpha(t) = u(t) = \beta(t)$.

The next theorem utilizes Type II coupled solutions, we obtain natural monotone sequences that converge uniformly and monotonically to the coupled minimal and maximal solutions of Type I of (4).

Theorem 4. Assume the following conditions hold
(C1) the functions v_0, w_0 are coupled lower and upper solutions of Type II for (4) satisfying $v_0 \le w_0$ for all $t \in \mathbb{T}$;
(C2) the functions $f1, f2 \in \mathscr{C}_{-\mathrm{rd}}\left(\mathbb{T}^\kappa \times \mathbb{R}^n, \mathbb{R}^n\right)$, $f_1(t,u)$ and $f_2(t,u)$ are non-decreasing in u for each $t \in \mathbb{T}$.

Then, there exist two monotone sequences $\{v_j(t)\}$ and $\{w_j(t)\}$ defined by

$$v_{j+1}{}^\Delta = f_1\left(t,v_j\right) - f_2\left(t,w_j\right),\ v_{j+1}\left(0\right) = u_0$$
$$w_{j+1}{}^\Delta = f_1\left(t,w_j\right) - f_2\left(t,v_j\right),\ w_{j+1}\left(0\right) = u_0,$$

satisfy the monotonicity property

$$v_0(t) \le v_1(t) \le \cdots \le v_j(t) \le w_j(t) \le \cdots \le w_1(t) \le w_0(t)$$
for all $t \in \mathbb{T}$

provided $v_0 \le v_1$ and $w_1 \le w_0$ on $\mathbb{T}$. Furthermore, the sequences $\{v_j(t)\}$ and $\{w_j(t)\}$ converge uniformly to $\alpha(t), \beta(t)$, respectively, where α, β are coupled minimal and maximal solutions of (4) such that they satisfy the coupled system,

$$\alpha^{\Delta} = f_1(t,\alpha) - f_2(t,\beta), \quad \alpha(0) = u_0$$
$$\beta^{\Delta} = f_1(t,\beta) - f_2(t,\alpha), \quad \beta(0) = u_0$$

for all $t \in \mathbb{T}$.

Remark 1. In Theorem 3,
(i) if $f_1(t,u) - f_2(t,u)$ is non-increasing on $\mathbb{T}$, then there exists a unique solution on $\mathbb{T}$.

(ii) if $f_2 \equiv 0$, then the conclusion of Theorem 3 is true.
Theorem 5. Assume that

(H1) v_0, w_0 are coupled lower and upper solutions of Type III for (4) with $v_0 \le u \le w_0$ on $t \in \mathbb{T}$;

(H2) $f_1, f_2 \in \mathscr{C}_{\mathrm{rd}}(\mathbb{T}^{\kappa} \times \mathbb{R}, \mathbb{R})$, $f_1(t,u)$ and $f_2(t,u)$ are nondecreasing in u for each $t \in \mathbb{T}$.

Then the sequences defined by

$$v_{j+1}{}^{\Delta} = f_1(t,w_j) - f_2(t,v_j),\ v_{j+1}(0) = u_0$$
$$w_{j+1}{}^{\Delta} = f_1(t,v_j) - f_2(t,w_j),\ w_{j+1}(0) = u_0.$$

give alternating monotone sequences $\{v_{2j}, w_{2j+1}\}$ and $\{w_{2j}, v_{2j+1}\}$ in $\mathscr{C}_{\mathrm{rd}}{}^{1}\left(\mathbb{T}, \mathbb{R}^n\right)$ where the sequences are given by

$$v_0 \le w_1 \le \cdots \le v_{2j} \le w_{2j+1} \le u \le v_{2j+1} \le w_{2j} \le \cdots \le v_1 \le w_0 \text{ on } \mathbb{T}$$

provided that $v_0 \le w_1 \le u \le v_1 \le w_0$ on $t \in \mathbb{T}$. Furthermore, the monotone sequences $\{v_{2j}, w_{2j+1}\}$ converge to α and $\{w_{2j}, v_{2j+1}\}$ converge to β, where α, β are coupled minimal and maximal solutions of (4) respectively, such that they satisfy the coupled system

$$\alpha^{\Delta} = f_1(t,\alpha) - f_2(t,\beta), \quad \alpha(0) = u_0$$
$$\beta^{\Delta} = f_1(t,\beta) - f_2(t,\alpha), \quad \beta(0) = u_0 \text{ on } \mathbb{T}.$$

Future research should extend this method to nonlinear functional dynamic equations. As this relatively new field continues to develop rapidly, significant opportunities exist for advancing both theoretical foundations and applications, particularly in hybrid dynamical systems.

References

1. Bhaskar TG, McRae FA. Monotone iterative techniques for nonlinear problems involving the difference of two monotone functions. Appl Math Comput. 2002; 133(1): 187-92.
2. Bohner M, Peterson A. Advances in dynamic equations on time scales. Boston, MA, Birkhäuser; 2003.
3. Denton Z, Vatsala AS. Monotone iterative technique for finite systems of nonlinear Riemann-Liouville fractional differential equations. Opuscula Math. 2011; 31(3): 327-39.
4. Kaymakçalan B. Existence and comparison results for dynamic systems on a time scale. J Math Anal Appl. 1993;172(1):243-55.
5. Kaymakçalan B. Monotone iterative method for dynamic systems on time scales. Dynam Systems Appl. 1993;2(2):213-20.
6. Ladde GS, Lakshmikantham V, Vatsala AS. Monotone iterative techniques for nonlinear differential equations. London: Pitman; 1985.
7. McRae FA. Monotone iterative technique and existence results for fractional differential equations. Nonlinear Anal. 2009;71(12):6093-6.
8. Ramírez JD, Vatsala AS. Generalized monotone iterative technique for Caputo fractional differential equation with periodic boundary condition via initial value problem. Int J Differ Equ. 2012;2012:1-17.
9. Wang WL, Tian JF. Generalized monotone iterative method for nonlinear boundary value problems with causal operators. Bound Value Probl. 2014;2014(1):192.
10. West IH, Vatsala AS. Generalized monotone iterative method for initial value problems. Appl Math Lett. 2004;17(11):1231-7.

HİTİT JOURNAL OF SCIENCE

e-ISSN: 3061-9629
Volume: 2 • Number: 2
July 2025

On the Eigenvalue Problems with Integrable Potential and Boundary Conditions Rationally Dependent on the Eigenparameter

Elif Başkaya

Department of Mathematics, Karadeniz Technical University, 61080, Trabzon, Türkiye.

Corresponding Author
Elif BAŞKAYA
E-mail: elifbekar@ktu.edu.tr Phone: +90 462 377 2569
RORID: ror.org/03z8fyr40

Article Information
Article Type: Research Article
Doi: -
Received: 31.05.2025
Accepted: 17.06.2025
Published: 31.07.2025

Cite As
Başkaya E. On the eigenvalue problems with integrable potential and boundary conditions rationally dependent on the eigenparameter. Hitit journal of Science. 2025;2(2):37-41.

Peer Review: Evaluated by independent reviewers working in at least two different institutions appointed by the field editor.
Ethical Statement: Not available.
Plagiarism Checks: Yes - iThenticate
Conflict of Interest: In this work, asymptotic expansions of the eigenvalues of an eigenvalue problem are calculated with better error terms than previous works.

CRedit Author Statement
Elif Başkaya: Design of the study, Conceptualization, Writing-original draft, Editing, Supervision.

On the Eigenvalue Problems with Integrable Potential and Boundary Conditions Rationally Dependent on the Eigenparameter

Elif Başkaya
Department of Mathematics, Karadeniz Technical University, 61080, Trabzon, Türkiye.

Abstract
We present the asymptotic estimates of the eigenvalues for an eigenvalue problem that the problem has also the eigenparameter in the second boundary condition, rationally. The potential of the problem is integrable.

Keywords: Asymptotic Estimates, Boundary Condition Rationally Dependent on the Eigenvalue, Eigenvalue Problem, Integrable Potential, Riccati Equation

INTRODUCTION

In this paper, we consider the following eigenvalue problem:

$$y''(t)+[\lambda-q(t)]y(t)=0, t\in[0,1] \quad (1)$$

$$y(0)\cos\alpha-y'(0)\sin\alpha=0, \alpha\in[0,\pi) \quad (2)$$

$$\frac{y'(1)}{y(1)}=s\left(\lambda\right)=\frac{h(\lambda)}{g(\lambda)} \quad (3)$$

where λ is a real parameter; the potential q is a real-valued L_1 function on the interval , also has a mean value zero, i.e. $\int_0^1 q\left(t\right)dt=0$; g and h are polynomials with real coefficients and no common zeros. When $\alpha=0$, the boundary condition Equation (2) is taken as $y(0)=0$ and when $s(\lambda)=\infty$ the boundary condition Equation (3) is accepted as $y(1)=0$. In addition, if $M=\deg(g)\geq\deg(h)$, let $h(\lambda)=A_M\lambda^M+\cdots+A_0$ where $A_M\in\mathbb{R}$ (it may be zero) and assume that g is monic, and if $\deg(g)<\deg(h)=M$, let $g(\lambda)=A_{M-1}\lambda^{M-1}+\cdots+A_0$ where $A_{M-1}\in\mathbb{R}$ (it may be zero) and assume that h is monic.

The above eigenvalue equation (1) are common to many areas of application. For example, Hooke' s law describes a mass on a spring as

$$F=-Kx$$

where K is the spring constant. Also, for the potential energy $V(x)$ of the spring, we have

$$V\left(x\right)=\frac{1}{2}Kx^2$$

and in classical mechanics we can write the force as

$$F=-\frac{\partial V}{\partial x}$$

The differential equation from Newton' s law as

$$m\ddot{x}=-Kx$$

or

$$\ddot{x}+\omega^2x=0$$

where $\omega^2=\frac{K}{m}$, Thus, the potential energy can be expressed as the following:

$$V\left(x\right)=\frac{1}{2}m\omega^2x^2$$

The time-independent Schrödinger equation for the one-dimensional simple harmonic oscillator is given as

$$\frac{-h^2}{2m}\frac{d^2\psi}{d^x2^2}+\frac{1}{2}mw^2x^2\psi=E\psi$$

or

$$\frac{d^2\psi}{\mathrm{d}x^2}+\left[\frac{2mE}{h^2}-\frac{m^2w^2x^2}{h^2}\right]\psi=0.$$

If we take $x:=t\sqrt{\frac{h}{m\omega}},\psi\left(x\right):=y\left(t\right)$ the Schrödinger equation becomes

$$y''\left(t\right)+\left[\lambda-t^2\right]y\left(t\right)=0 \quad (4)$$

where $\lambda=\frac{2E}{hw}$ is the dimensionless energy. Equation (4) is an eigenvalue equation in the form of Equation (1).

The problem Equation (1)-Equation (3) is different from the usual regular eigenvalue problem because eigenvalue parameter λ is held in the second boundary condition. Such problems often arise from physical problems, quantum mechanics and geophysics and are studied by a lot of researchers. Some of them are [1]-[16]. We especially refer to [1], [13] and [16]. In [1], the asymptotic eigenvalues of the problem Equation (1)-Equation (3) with $q\in \mathrm{AC}\left[0,1\right]$ are given and it is shown that the Weyl m-function uniquely determines α, f and q; and is in turn uniquely determined by either two spectra from different values of α or by the Prüfer angle. In [13], the asymptotic eigenfunctions of the problem Equation (1)-Equation (3) with $q\in L_1\left[0,1\right]$ are found. And [16] introduces the inverse problem associated with the problem Equation (1)-Equation (3) by providing the eigenvalues and the corresponding eigenfunctions to uniquely determine the potential $q(t)$ that is be a continuously differentiable function on .

Our aim is to obtain asymptotic expansions of the eigenvalues of the problem Equation (1)-Equation (3) with better error terms than previous works.

MATERIAL AND METHODS

Our method is based on [7]. Let us associate Equation (1) with the Riccati equation

$$v'\left(t,\lambda\right)=-\lambda+q-v^2$$

and define

$$S(t,\lambda):=\mathrm{Re}[v(t,\lambda)], \quad (5)$$

$$T(t,\lambda) := \operatorname{Im}[v(t,\lambda)]. \tag{6}$$

It is shown in [7] that any real-valued solution of Equation (1) is in the form

$$y(t,\lambda) = R(t,\lambda)\cos\theta(t,\lambda)$$

with

$$S\left(t,\lambda\right) = \frac{R'(t,\lambda)}{R(t,\lambda)}, \tag{7}$$

$$T\left(t,\lambda\right) = \theta'\left(t,\lambda\right). \tag{8}$$

Our approach to calculating λ_n is to approximate λ those which are such that

$$\theta\left(1,\lambda\right) - \theta\left(0,\lambda\right) = \int_0^1 T\left(x,\lambda\right)dx$$

We suppose that there exist functions $A(t)$ and $\eta(\lambda)$ so that

$$\left|\int_t^1 e^{2i\sqrt{\lambda}x}q\left(x\right)dx\right| \le A\left(t\right)\eta\left(\lambda\right), t\in[0,1]$$

where

i) $A\left(t\right) := \int_t^1 \left|q\left(x\right)\right|dx$ is a decreasing function of

ii) $A(t)\in L[0,1]$,

iii) $\eta(\lambda)\to 0$ as $\lambda\to\infty$.

For $q\in L[0,1]$ the existence of the functions A and η may be established for λ positive as follows. It is clear that $\left|\int_t^1 e^{2i\sqrt{\lambda}x}q\left(x\right)dx\right| \le \int_t^1\left|q\left(x\right)\right|dx \le \infty$ hence, if we define

$$F\left(t,\lambda\right) := \begin{cases} \dfrac{\left|\int_t^1 e^{2i\lambda^{1/2}x}q\left(x\right)dx\right|}{\int_t^1\left|q\left(x\right)\right|dx} & \text{if } \int_t^1\left|q\left(x\right)\right|dx \ne 0 \\ 0 & \text{if } \int_t^1\left|q\left(x\right)\right|dx = 0 \end{cases} \tag{9}$$

we gain $0\le F(t,\lambda)\le 1$. Also, if we set $\eta\left(\lambda\right) := \sup_{a\le t\le b} F\left(t,\lambda\right)$ we have $\eta(\lambda)$ is well defined by Equation (9) and $\eta(\lambda)\to 0$ as $\lambda\to\infty$ [7].

Our method of approximating a solution of $v'(t,\lambda) = -\lambda + q - v^2$ on [0,1] is similar to [7], so we set

$$v\left(t,\lambda\right) := i\lambda^{1/2} + \sum_{n=1}^{\infty} v_n\left(t,\lambda\right). \tag{10}$$

When we put this serie into the Riccati equation and solve differential equations, we hold

$$v_1\left(t,\lambda\right) = -e^{-2i\lambda^{1/2}t}\int_t^1 e^{2i\lambda^{1/2}x}q\left(x\right)dx,$$

$$v_2\left(t,\lambda\right) = e^{-2i\lambda^{1/2}t}\int_t^1 e^{2i\lambda^{1/2}x}{v_1}^2\left(x,\lambda\right)dx,$$

for $n\ge 3$

$$v_n\left(t,\lambda\right) = e^{-2i\lambda^{1/2}t}\int_t^1 e^{2i\lambda^{1/2}x}\left[{v_{n-1}}^2\left(x,\lambda\right) + 2v_{n-1}\left(x,\lambda\right)\sum_{m=1}^{n-2}v_m\left(x,\lambda\right)\right]dx.$$

Also from Equation (6), Equation (8) and Equation (10), we have $\theta\left(1,\lambda\right) - \theta\left(0,\lambda\right) = \int_0^1\left[\lambda^{1/2} + \operatorname{Im}\sum_{n=1}^{\infty}v_n(x,\lambda)\right]dx$, then $\theta\left(1,\lambda\right) - \theta\left(0,\lambda\right) = \lambda^{1/2} + \sum_{n=1}^{\infty}\operatorname{Im}\int_0^1 v_n\left(x,\lambda\right)dx$ and from this equation, [2] proves that

$$\theta\left(1,\lambda\right) - \theta\left(0,\lambda\right) = \lambda^{1/2} - \tfrac{1}{2}\lambda^{-1/2}\int_0^1 q\left(x\right)\left[\cos 2\lambda^{1/2}x\right]dx + O\left(\lambda^{-1}\eta\left(\lambda\right)\right) \tag{11}$$

Let us consider the following theorem:

Theorem: [2] If $v(t,\lambda)$ as in (2.6), as $\lambda\to\infty$

$$v(t,\lambda) = i\lambda^{1/2} + v_1(t,\lambda) + O(\eta^2(\lambda))$$

where

$$v_1(t,\lambda) = \left[\operatorname{isin}(2\lambda^{1/2}t) - \cos(2\lambda^{1/2}t)\right]$$

$$\times\int_t^b\left[\cos(2\lambda^{1/2}x) + \operatorname{isin}(2\lambda^{1/2}x)\right]q\left(x\right)dx + O\left(\eta^2\left(\lambda\right)\right).$$

After some calculations by using the last theorem, with Equation (5) we gain

$$S(t,\lambda) = -\sin(2\lambda^{1/2}t + \xi_t) + O(\eta^2(\lambda)) \tag{12}$$

where

$$\sin\xi_t := \int_t^1\left(\cos 2\lambda^{1/2}x\right)q\left(x\right)dx,$$

$$\cos\xi_t \;:= \int_t^1\left(\sin 2\lambda^{1/2}x\right)q\left(x\right)dx.$$

Similarly, with Equation (6) we find $T(t,\lambda)$ as

$$T\left(t,\lambda\right) = \lambda^{1/2} - \cos\left(2\lambda^{1/2}t + \xi_t\right) + O\left(\eta^2(\lambda)\right) \tag{13}$$

so we can write

$$S\left(0,\lambda\right) = -\int_0^1\left(\cos 2\lambda^{1/2}x\right)q\left(x\right)dx + O\left(\eta^2\left(\lambda\right)\right), \tag{14}$$

$$T\left(0,\lambda\right) = \sqrt{\lambda} - \int_0^1\left(\sin 2\sqrt{\lambda}x\right)q\left(x\right)dx + O\left(\eta^2\left(\lambda\right)\right), \tag{15}$$

$$S(1,\lambda) = O(\eta^2(\lambda)), \tag{16}$$

$$T\left(1,\lambda\right) = \lambda^{\frac{1}{2}} + O\left(\eta^2\left(\lambda\right)\right). \tag{17}$$

RESULTS AND DISCUSSION

We approximate the eigenvalues of the problem Equation (1)-Equation (3), in this section. It is shown in [7] that any real valued solution $y(t,\lambda)$ of Equation (1) is of the form

$$y(t,\lambda) = R(t,\lambda)\cos\theta(t,\lambda), \tag{18}$$

hence

$$y'\left(t,\lambda\right) = R'\left(t,\lambda\right)\cos\theta\left(t,\lambda\right) - R\left(t,\lambda\right)\theta'\left(t,\lambda\right)\sin\theta\left(t,\lambda\right). \tag{19}$$

We now determine the conditions under which the first boundary condition Equation (2) and the second boundary condition Equation (3) are satisfied.

Considering Equation (18) and Equation (19), one observes that Equation (2) holds if

$$R\left(0,\lambda\right)\left\{\cos\theta\left(0,\lambda\right)\left[\cos\alpha - \frac{R'}{R}\left(0,\lambda\right)\sin\alpha\right] + \sin\theta\left(0,\lambda\right)\theta'\left(0,\lambda\right)\sin\alpha\right\} = 0. \tag{20}$$

i) For $\alpha \neq 0$:
We can write Equation (20) as

$R(0,\lambda)\cdot \sin\left[\theta(0,\lambda)-\gamma_1\right]=0$

where

$$\sin\gamma_1 := \frac{R'(0,\lambda)}{R(0,\lambda)}\cdot \sin\alpha - \cos\alpha,$$

$$\cos\gamma_1 := \theta'(0,\lambda)\cdot\sin\alpha.$$

From Equation (7) and Equation (8)

$$\sin\gamma_1 = S(0,\lambda)\cdot\sin\alpha-\cos\alpha, \tag{21}$$

$$\cos\gamma_1 = T(0,\lambda)\cdot\sin\alpha \tag{22}$$

And we also from Equation (20)

$$\theta(0,\lambda)=\gamma_1. \tag{23}$$

Substituting the values of $S(0,\lambda)$ and $T(0,\lambda)$ given by Equation (14) and Equation (15) into Equation (21) and Equation (22), one obtains

$$\frac{\sin\gamma_1}{\cos\gamma_1} = \frac{-\cos\alpha-\sin\alpha\int_0^1(\cos 2\lambda^{1/2}x)q\left(x\right)dx+O\left(\eta^2\left(\lambda\right)\right)}{\lambda^{1/2}\sin\alpha-\sin\alpha\int_0^1(\sin 2\lambda^{1/2}x)q\left(x\right)dx+O\left(\eta^2\left(\lambda\right)\right)}$$

$$=\frac{-\cos\alpha-\sin\alpha\int_0^1\cos 2\sqrt{\lambda}xq\left(x\right)dx+O\left(\eta^2\left(\lambda\right)\right)}{\sqrt{\lambda}\sin\alpha\cdot\left[1-\lambda^{-\frac{1}{2}}\int_0^1\sin 2\sqrt{\lambda}xq\left(x\right)dx+\mathrm{O}\left(\lambda^{-\frac{1}{2}}\cdot\eta^2\left(\lambda\right)\right)\right]}$$

and

$$\frac{\sin\gamma_1}{\cos\gamma_1}=\left\{-\lambda^{-\frac{1}{2}}\cot\alpha-\lambda^{-\frac{1}{2}}\int_0^1\cos 2\sqrt{\lambda}xq\left(x\right)dx+\mathrm{O}\left(\lambda^{-\frac{1}{2}}\eta^2\left(\lambda\right)\right)\right\}$$

$$\times\left\{1+\lambda^{-\frac{1}{2}}\int_0^1\sin 2\sqrt{\lambda}xq\left(x\right)dx+\mathrm{O}\left(\lambda^{-\frac{1}{2}}\eta^2\left(\lambda\right)\right)\right\}$$

so

$$\tan\gamma_1=-\lambda^{-1/2}\cot\alpha-\lambda^{-1/2}\int_0^1\left(\cos 2\lambda^{1/2}x\right)q\left(x\right)dx+O\left(\left(\lambda^{-1/2}\eta\right)^2\left(\lambda\right)\right) \tag{24}$$

ii) For $\alpha=0$
In this case, Equation (20) reduces
$R(0,\lambda)\cos\theta(0,\lambda)=0$

and from this equation, the first boundary condition Equation (2) is satisfied for

$$\theta\left(0,\lambda\right)=\frac{\pi}{2}.$$

Considering Equation (18) and Equation (19), one observes that the second boundary condition Equation (3) holds if

$$R\left(1,\lambda\right)\left\{\cos\theta\left(1,\lambda\right)\left[h\left(\lambda\right)-\frac{R\prime(1,\lambda)}{R(1,\lambda)}g\left(\lambda\right)\right]+\sin\theta\left(1,\lambda\right)\theta\prime\left(1,\lambda\right)g\left(\lambda\right)\right\}=0 \tag{26}$$

iii) For $\deg(h)\leq\deg(g)=M$:

The Equation (26) is expressed as

$$R(1,\lambda)\sin\left[\theta(1,\lambda)-\gamma\_2\right]=0 \tag{27}$$

where

$$\sin\gamma_2 := \frac{R'(1,\lambda)}{R(1,\lambda)}g\left(\lambda\right)-h\left(\lambda\right),$$

$$\cos\gamma_2 := \theta'\left(1,\lambda\right)g\left(\lambda\right).$$

From the definitions of $g(\lambda)$ and $h(\lambda)$ one writes

$$\sin\gamma_2=S(1,\lambda)\left[\lambda^M+B_{M-1}\lambda^{M-1}+\cdots+B_0\right]-\left[A_M\lambda^M+A_{M-1}\lambda^{M-1}+\cdots+A_0\right]$$
$$\cos\gamma_2=T\left(1,\lambda\right)\left[\lambda^M+B_{M-1}\lambda^{M-1}+\cdots+B_0\right]$$

and substitution of Equation (16) and Equation (17) into the last equations gives

$$\sin\gamma_2=-A_M\lambda^M+\mathrm{O}\left(\lambda^M\eta^2(\lambda)\right),$$
$$\cos\gamma_2=\lambda^{M+\frac{1}{2}}+\mathrm{O}\left(\lambda^M\eta^2(\lambda)\right)$$

hence

$$\frac{\sin\gamma_2}{\cos\gamma_2}=\frac{-A_M\lambda^M+\mathrm{O}\left(\lambda^M\eta^2\right)}{\lambda^{M+\frac{1}{2}}+\mathrm{O}\left(\lambda^M\eta^2\right)}=\frac{-A_M\lambda^M+\mathrm{O}\left(\lambda^M\eta^2\right)}{\lambda^{M+\frac{1}{2}}\left[1+\mathrm{O}\left(\lambda^{-\frac{1}{2}}\eta^2\right)\right]}$$

$$=\left\{-A_M\lambda^{-\frac{1}{2}}+\mathrm{O}\left(\lambda^{-\frac{1}{2}}\eta^2\left(\lambda\right)\right)\right\}\cdot\left\{1-\mathrm{O}\left(\lambda^{-\frac{1}{2}}\eta^2\left(\lambda\right)\right)\right\}$$

then

$$\tan\gamma_2=-A_M\lambda^{-\frac{1}{2}}+\mathrm{O}\left(\lambda^{-\frac{1}{2}}\eta^2\left(\lambda\right)\right). \tag{28}$$

Also from Equation (27), we have

$$\theta(1,\lambda)=(n+1)\pi+\gamma_2 \tag{29}$$

iv) For $\deg(g)<\deg(h)=M$:

The Equation (26) is obtained as
$R(1,\lambda)\sin\left[\theta(1,\lambda)-\gamma_3\right]=0$

where

$$\sin\gamma_3 := \frac{R\prime(1,\lambda)}{R(1,\lambda)}g\left(\lambda\right)-h\left(\lambda\right),$$

$$\cos\gamma_3 := \theta'(1,\lambda)g(\lambda)$$

so that

$$\theta(1,\lambda)=(n+1)\pi+\gamma_3 \tag{30}$$

From the definitions of and one writes

$$\sin\gamma_3=S\left(1,\lambda\right)\left[A_{M-1}\lambda^{M-1}+A_{M-2}\lambda^{M-2}+\cdots+A_0\right]$$

$$-\left[\lambda^M+B_{M-1}\lambda^{M-1}+\cdots+B_0\right]$$

$$\cos\gamma_3=T\left(1,\lambda\right)\left[A_{M-1}\lambda^{M-1}+A_{M-2}\lambda^{M-2}+\cdots+A_0\right]$$

and substitution of Equation (16) and Equation (17) into the last equations gives

$$\sin\gamma_3=-\lambda^M-B_{M-1}\lambda^{M-1}+O\left(\lambda^{M-1}\eta^2(\lambda)\right)$$

$$\cos\gamma_3=A_{M-1}\lambda^{M-\frac{1}{2}}+O\left(\lambda^{M-1}\eta^2\left(\lambda\right)\right),$$

thus

$$\frac{\cos\gamma_3}{\sin\gamma_3}=\frac{A_{M-1}\lambda^{M-\frac{1}{2}}+O\left(\lambda^{M-1}\eta^2\left(\lambda\right)\right)}{-\lambda^M-B_{M-1}\lambda^{M-1}+O(\lambda^{M-1}\eta^2(\lambda))}$$

$$=\frac{A_{M-1}\lambda^{M-\frac{1}{2}}+O\left(\lambda^{M-1}\eta^2\left(\lambda\right)\right)}{-\lambda^M(1+B_{M-1}\lambda^{-1}+O(\lambda^{-1}\eta^2(\lambda)))}$$

then

$$\cot\gamma_3=-A_{M-1}\lambda^{-\frac{1}{2}}+O\left(\lambda^{-1}\eta^2\left(\lambda\right)\right) \tag{31}$$

Theorem: The asymptotic formulae for the eigenvalues of the problem Equation (1)-Equation (3) satisfy, as $n\to\infty$

(i) if $\alpha\neq 0$ and $\deg(h)\leq\deg(g)=M$,

$$\lambda_n^{1/2}=\left(n+1\right)\pi+\frac{1}{(n+1)\pi}\left[-A_M+\cot\alpha+\frac{3}{2}\int_0^1 q\left(x\right)\cos\left(2\left(n+1\right)\pi x\right)dx\right]$$
$$+O\left(n^{-1}\eta^2\left(n\right)\right)+O\left(n^{-2}\eta\left(n\right)\right)$$

(ii) if $\alpha\neq 0$ and $\deg(g)<\deg(h)=M$,

$$\lambda_n^{1/2}=\frac{2n+3}{2}\pi+\frac{2}{2n+3\pi}\left[A_{M-1}+\cot\alpha+\frac{3}{2}\int_0^1 q\left(x\right)\cos\left((2n+3)\pi x\right)dx\right]$$
$$+O\left(n^{-1}\eta^2\left(n\right)\right)+O\left(n^{-2}\eta\left(n\right)\right)$$

(iii) if $\alpha=0$ and $\deg(h)\leq\deg(g)=M$,

$$\lambda_n^{1/2}=\frac{2n+1}{2}\pi+\frac{2}{2n+1\pi}\left[-A_M+\frac{1}{2}\int_0^1 q\left(x\right)\cos\left((2n+1)\pi x\right)dx\right]$$
$$+O\left(n^{-1}\eta^2\left(n\right)\right)+O\left(n^{-2}\eta\left(n\right)\right)$$

(iv) if $\alpha=0$ and $\deg(g)<\deg(h)=M$,

$$\lambda_n^{1/2}=\left(n+1\right)\pi+\frac{1}{(n+1)\pi}\left[A_{M-1}+\frac{1}{2}\int_0^1 q\left(x\right)\cos\left(2\left(n+1\right)\pi x\right)dx\right]$$
$$+O\left(n^{-1}\eta^2\left(n\right)\right)+O\left(n^{-2}\eta\left(n\right)\right)$$

Proof: Theorem (i) is proved by using Equation (11), Equation (23), Equation (24), Equation (28), Equation (29) together with inverse trigonometric series and reversion. Theorem (ii) is proved by using Equation (11), Equation (23), Equation (24), Equation (30), Equation (31) together with inverse trigonometric series and reversion. Theorem (iii) is proved by using Equation (11), Equation (25), Equation (28), Equation (29) together with inverse trigonometric serie and reversion. Theorem (iv) is proved by using Equation (11), Equation (25), Equation (30), Equation (31) together with inverse trigonometric serie and reversion.

CONCLUSION

In this work, asymptotic expansions of the eigenvalues of an eigenvalue problem are calculated with better error terms than previous works.

References

1. Binding P. A., Browne P. J. and Watson B. A., 2004. Equivalence of Inverse Sturm-Liouville Problems with Boundary Conditions Rationally Dependent on the Eigenparameter. Journal of Mathematical Analysis and Applications, 291, 246-261.
2. Coşkun H. and Başkaya E., 2010. Asymptotics of eigenvalues for regular Sturm-Liouville problems with eigenvalue parameter in the boundary condition for integrable potential. Mathematica Scandinavica, 107, 209-223.
3. Coşkun H., Başkaya E. and Kabataş A., 2019. Instability intervals for Hill's equation with symmetric single well potential. Ukrainian Mathematical Journal, 71 (6), 977-983.
4. Coşkun H. and Kabataş A., 2013. Asymptotic approximations of eigenfunctions for regular Sturm-Liouville problems with eigenvalue parameter in the boundary condition for integrable potential. Mathematica Scandinavica, 113 (1), 143-160.
5. Coşkun H. and Kabataş A., 2016. Green's function of regular Sturm-Liouville problem having eigenparameter in one boundary condition. Turkish Journal of Mathematics and Computer Science, 4, 1–9.
6. Coşkun H., Kabataş A. and Başkaya E., 2017. On Green's function for boundary value problem with eigenvalue dependent quadratic boundary condition. Boundary Value Problems, 71.
7. Harris B. J., 1997. The Form of the Spectral Functions Associated with Sturm-Liouville Problems with Continuous Spectrum. Mathematika, 44 (1), 149-161.
8. Kabataş A., 2022. On eigenfunctions of Hill' s equation with symmetric double well potential. Communications Faculty of Sciences University of Ankara-Series A1 Mathematics and Statistics, 71 (3), 634-649.
9. Kabataş A., 2022. Eigenfunction and Green' s function asymptotics for Hill' s equation with symmetric single-well potential. Ukrainian Mathematical Journal, 74 (2), 218-231.
10. Kabataş A., 2023. One boundary value problem including a spectral parameter in all boundary conditions. Opuscula Mathematica, 43 (5), 651-661.
11. Kabataş A., 2023. Sturm-Liouville problems with polynomially eigenparameter dependent boundary conditions. Sakarya University Journal of Science, 27 (6), 1235-1242.
12. Kabataş A., 2023. Sturm-Liouville problems including boundary conditions polynomially dependent on the eigenparameter with differentiable potential. International Research and Reviews in Science and Mathematics, Serüven Publishing, Ankara, 1-16.
13. Kabataş A., 2023. On eigenfunctions of the Sturm-Liouville problems with boundary conditions rationally dependent on the eigenparameter. International Theory, Research and Reviews in Science and Mathematics, Serüven Publishing, Ankara, 263-281.
14. Kabataş A., 2023. On Sturm-Liouville problems including the square-root of the eigenvalue parameter in one boundary condition. New Frontiers in Natural Science and Mathematics, Duvar Publishing, İzmir, 233-251.
15. Kabataş A., 2024. Green's function asymptotics for a boundary value problem contained eigenvalue parameter in the boundary condition. Advances in Mathematics Research Volume 35, NOVA Science Publishers Inc. , New York, 43-53.
16. Mosazadeh S. and Akbarfam A. J., 2020. Inverse and Expansion Problems with Boundary Conditions Rationally Dependent on the Eigenparameter. Bulletin of the Iranian Mathematical Society, 46, 67-78.

HİTİT JOURNAL OF SCIENCE

e-ISSN: 3061-9629
Volume: 2 • Number: 2
July 2025

The Role of Fingernail DNA in Forensic Science

Esra Betül Peksak[1,*] | Sabiha Şensöz[2]

[1]Department of Forensic Sciences Hitit University, 19030, Corum, Türkiye.
[2]Department of Nutrition and Dietetics Hitit University, 19030, Corum, Türkiye.

Corresponding Author

Esra Betül PEKSAK
E-mail: 240421015@ogrenci.hitit.edu.tr Phone: +90 552 559 97 98
RORID: ror.org/01x8m3269

Article Information

Article Type: Review
Doi: -
Received: 30.04.2025
Accepted: 07.07.2025
Published: 31.07.2025

Cite As

Peksak EB., Şensöz S. The Role of Fingernail DNA in Forensic Science. Hitit journal of Science. 2025;2(2):42-53.

Peer Review: Evaluated by independent reviewers working in at least two different institutions appointed by the field editor.
Ethical Statement: Not available.
Plagiarism Checks: Yes - iThenticate
Conflict of Interest: Authors approve that to the best of their knowledge, there is not any conflict of interest or common interest with an institution/organization or a person that may affect the review process of the paper.
Acknowledgements: The author received no financial support for the research, authorship, and/or publication of this article.

CRedit Author Statement
Esra Betül Peksak: Design of the study, Conceptualization, Writing-original draft, Editing **Sabiha Şensöz:** Design of the study, Supervision.

The Role of Fingernail DNA in Forensic Science

Esra Betül Peksak[1,*] | Sabiha Şensöz[2]
[1]Department of Forensic Sciences Hitit University, 19030, Corum, Türkiye.
[2]Department of Nutrition and Dietetics Hitit University, 19030, Corum, Türkiye.

Abstract
Forensic genetics significantly contributes to the resolution of various criminal cases. In addition to DNA typing, nail samples and biological materials collected from underneath the fingernails are crucial sources of evidence, especially in cases involving violence and physical struggle. Consequently, various techniques have been developed for DNA isolation from both nails and undernail materials, yet there is no consensus regarding the most effective method. Factors such as the collection technique, daily activities, transfer of material, and the presence of mixed DNA profiles significantly influence the forensic reliability of these samples. Moreover, it remains unclear whether direct analysis of nail tissue or swab samples from under the nails is more effective, or whether swabs should be collected using dry or damp cotton. There is also debate over whether nail tissues and undernail swabs should be analyzed separately or together. Additionally, forensic laboratories lack standardized protocols for the storage and transport of these samples. This study explores the forensic value and analysis methods of nail and undernail materials based on current research. This review article will review studies on nail samples. It will describe the most effective nail sample collection method by presenting a review of studies. It aims to provide information on how fingernails can be analyzed in forensic science. The methods used to analyze fingernail samples will be described in detail to provide an overview for those browsing this review article.

Keywords: Forensic DNA analysis, forensic genetic, fingernail material, swab

INTRODUCTION
BIOLOGICAL EVIDENCE: NAILS

During acts of violence such as homicide, sexual assault, or other physical confrontations, the struggle between victim and perpetrator often results in the exchange of biological traces (Nurit et al., 2011) (see Figure 1). Among the transferred biological evidence (including epithelial cells, blood, and hair) material can accumulate under the victim's fingernails. Although the exact nature and extent of physical contact necessary for this transfer is not fully established, post-incident DNA analysis has proven to be instrumental in suspect identification (Ea et al., 2010).

Figure 1. Forensic sampling of fingernail material using a cotton swab.

In addition, everyday physical contact may result in the deposition of biological debris beneath the fingernails. While such accumulation typically does not yield complex or detectable DNA mixtures, it may contain trace amounts of extraneous DNA, often originating from a person with whom the individual has close physical contact, such as a partner (Cook and Dixon, 2007). Studies have shown that the rate of detecting foreign DNA in such instances can range from 6% to 17% (Cook and Dixon, 2007; Malsom et al., 2009).

However, in cases involving homicide or sexual violence, the nature of the interaction is often forceful and prolonged, increasing the likelihood of recovering foreign DNA from subungual material, which can provide crucial evidence for case resolution (Cook and Dixon, 2007; Piccinini, 2003). Particularly in postmortem investigations, since the deceased cannot remove biological material themselves, and unless it is eliminated by environmental conditions or the perpetrator, foreign DNA is likely to persist under the fingernails and serve as valuable forensic evidence (Nurit et al., 2011).

As is well-established in forensic genetics, determining whether a biological trace belongs to the perpetrator requires compatibility between the DNA profile obtained from the evidence and the reference sample, particularly in terms of standardized polymorphic autosomal short tandem repeat (STR) loci (Butler, 2007). In cases involving sexual assault, where male and female DNA are often mixed, Y-chromosome analysis can facilitate the identification of male DNA. Y-STR profiling offers a significant advantage when male DNA is masked by an excess of female DNA, allowing for the detection of a male-specific profile that may not be discernible via autosomal STRs (Cerri et al., 2007). The analysis results obtained from such case studies need to be confirmed by alternative methods (Karadayı et al., 2021).

CHARACTERISTICS OF NAIL MATERIAL AND IMPORTANCE OF THE NAIL IN FORENSIC CASES

Nails are highly resistant to decay, and both they and the tissues around them are a rich source of DNA. Despite various environmental influences, such as burial or exposure to water, DNA typing can be performed from nails (Watherston et al, 2018). Especially in cases of violent crimes and sexual assault, nail marks can be found on the bodies of victims or perpetrators (Shimamoto et al., 2013). Comparison can be made by examining the shapes of the nail marks or the dimensions of the openings between the fingers. Fragments left at the crime scene as a result of damage to nails due to factors such as breaking or cutting allow evidence to be matched and compared with its source (Bengtsson et al., 2012; Roux et al., 2015). When the fingers are pressed vertically, when they touch somewhere, the nail marks may have sharp edges and a moon-shaped. Especially when slid vertically on the human body, it leaves road-like scars. Clear shapes may occur at the end point of these traces. Suspects can be identified through detection and matching. In addition, residues such as hair, hair, fibers, blood, skin, prohibited substances between the nails can be examined by biological and chemical analyzes and important information about the person, event or suspect can be obtained (Cavus et al., 2024). For this reason, DNA analysis under the nails is of great importance in terms of identifying the culprits and clarifying the events (Nurit et al, 2011). If the suspect scratches, there is a high probability that there is blood and epidermal tissue under the victim's nails. Therefore, tissue samples under the nail should be taken with a sterile toothpick and the nails should be cut and placed in the evidence envelope (Dowlman et al., 2010; De Bruin et al., 2012; Newton et al., 2013).

COLLECTION OF NAIL SAMPLES AND DNA ANALYSIS IN FORENSIC GENETICS

STR ANALYSIS

Today's forensic genetics and frequently analyzed genetic polymorphisms are STR regions that were included in case studies in the late 1990s. (Edwards et al., 1991) STRs (Short Tandem Repeats), commonly used in forensic genetics and known as short tandem repeats, are a type of genetic polymorphism. With 22 autosomal chromosomes, thousands of STR regions located on the X and Y chromosomes can be analyzed (Butler, 2011). STR, or short sequential repeat sequences, are repetitive polymorphic DNA sequences of 2-6 bases in length (Brinkmann, 1992). While many methods such as VNTR and RFLP are insufficient, reliable results can be obtained with STR loci because forensic samples are generally highly fragmented, their molecular structure is degraded and the amount of DNA is less than 100 nanograms, (Alford et al., 1994). There are two alleles belonging to each STR locus in the human genome. One comes from the mother and the other from the father. STR analysis is based on repeat variation of STR loci between individuals. Today, techniques based on the amplification of STR loci by PCR method are used in forensic DNA analysis. Polymorphic STR loci are available in kit form under trademarks (Budowle and Van Daal, 2008).

Y-STR ANALYSIS

Unlike autosomal STR regions, short repeat sequences (Y-STRs) on the Y chromosome, which are only found in male individuals, have gained an important use in forensic DNA analysis in recent years. Except for a small region of the Y chromosome containing autosomal genes, the rest of the Y chromosome does not undergo recombination during meiosis. Therefore, Y-STRs are transmitted unchanged from father to son from generation to generation as linked haplotypes. This makes Y-STR analyses particularly valuable in lineage tracing, anthropological research and paternity testing when the father is unavailable.

One important aspect that must not be overlooked when analyzing fingernail samples is the gender of the victim and the suspect. In cases where the victim is female and the suspect is male, performing a Y-STR analysis on DNA material collected from underneath the victim's fingernails can be critical in elucidating the incident. The small amount of male DNA transferred to the victim's fingernails may be masked by the predominant female DNA during autosomal STR analysis. However, Y-STR analysis allows for the specific detection of male DNA, enabling the identification of otherwise obscured genetic material and contributing significantly to the investigation (Iuvaro et al., 2018).

Due to the advantages of Y-STR analysis, it has been widely used in recent years, and many studies have been carried out to demonstrate its diversity in different populations and its discriminative power in identification (Kayser, 2017).

X-STR ANALYSIS

The discriminatory power (PD) of X chromosome markers in biological evidence varies depending on the sex of the individual being compared. When comparing samples from two females, the PD value of X-linked markers is equivalent to that of autosomal markers. However, when male biological material is compared with that of another male, the PD value of X-linked markers is lower than that of autosomal markers because males have only one X chromosome. In mixed samples, Y-STR analysis is preferred to detect the presence of a male, while X-STR markers can be more effective than autosomal STRs in identifying the presence of a female. This is because, unless all X-STR loci are homozygous, two alleles can be observed in an individual (Szibor, 2007).

In paternity cases, autosomal STRs are generally sufficient because there is no X chromosome inheritance between father and son; therefore, X-STRs are not used in father-son relationships. However, in father-daughter cases, since the daughter inherits one X chromosome from the father, X-STR analysis can be considered as a supplement to autosomal STRs (Szibor et al., 2003; Pereira et al., 2007).

In cases involving male relatives such as father and son, if the child is female, X-STR analysis can be used for paternity testing because fathers with different mothers possess different X chromosomes (Szibor, 2007). However, in paternity analysis of brothers, X-STR effectiveness decreases by about 50% due to a shared mother, making it less preferable.

Consequently, the literature contains very few studies addressing X-STR methods for nail samples.

NGS (Next-Generation Sequencing)

The NGS (Next-Generation Sequencing) method used in the analysis of nail samples offers comprehensive and highly sensitive genetic examination, especially in samples containing low amounts of degraded DNA. Nails are among the biological materials resistant to DNA degradation, but they generally provide limited amounts of DNA. Compared to traditional analysis methods, NGS technology has the capability to analyze numerous genetic regions simultaneously, with deep coverage and high accuracy. NGS enables the simultaneous examination of genetic markers such as STRs (Short Tandem Repeats) and SNPs (Single Nucleotide Polymorphisms) on both nuclear and mitochondrial DNA isolated from nails. This feature allows for more reliable and detailed results, particularly in complex and mixed DNA samples. Furthermore, NGS can sequence even small amounts of DNA found in nail samples, making it an important tool in forensic science, identification, and lineage tracing. In summary, the NGS method provides comprehensive and highly accurate evaluation of both nuclear and mitochondrial DNA in nail samples, offering an effective and reliable solution in forensic analyses where traditional techniques fall short (Preuner et al., 2014).

mt-DNA

One of the situations frequently encountered in forensic sciences is that the amount of nuclear DNA in samples arriving at the laboratory is insufficient or the DNA is excessively fragmented due to environmental factors. In such cases, reliable results may not be obtained from classical STR (Short Tandem Repeat) analyses. Especially in biological samples that have been exposed to direct sunlight for a long time, stored in high humidity environments or found in acidic soil, nuclear DNA integrity is seriously impaired. In such cases, mitochondrial DNA (mtDNA) analyses come to the fore as an alternative molecular approach (Wilson MR et al., 1995; Allen M et al., 1998; Steighner RJ and Holland M, 1998).

The main feature that makes mitochondrial DNA so important and valuable in forensic genetics is that it has hundreds or even thousands of copies per cell (Robin ED and Wong R, 1988). However, the autosomal chromosomes found in the nuclear genome are in only two copies. This difference makes mtDNA a valuable alternative, especially when nuclear DNA cannot be obtained or analyzed. For example, in samples such as shed hair without hair follicles, bone, nail and tooth samples exposed to extreme environmental conditions such as long-term high temperature and humidity, deteriorated tissues or old biological stains, even a few intact copies of mtDNA can allow successful analysis (Melton T and Nelson K, 2001; Melton T et al., 2005; Hopwood AJ et al., 1996).

Another important feature of mtDNA is that it shows maternal inheritance, that is, it is transmitted from generation to generation only through the mother (Giles RE et al., 1980). This means that all individuals from the same maternal lineage will have essentially the same mtDNA profile. Therefore, in cases where identification is required, an individual's mtDNA profile can be directly compared to the profiles of their mother or maternal relatives. In the absence of mutations, the mtDNA sequences of these individuals will be identical.

This feature is particularly valuable in mass casualty cases where identification is difficult, such as natural disasters, plane crashes, large explosions, mass murders, war crimes, and terrorist incidents. In such cases, identification may not be possible with classical methods due to factors such as excessive damage to the bodies, unrecognizable bodies, or separation of body parts. However, by comparing the mtDNA profile with samples from close relatives on the mother's side, the identities of these individuals can be successfully determined (Goodwin W et al., 1999).

In conclusion, mtDNA analyses are used as a reliable and powerful method in forensic sciences, especially in cases where nuclear DNA cannot be analyzed or found, thanks to both technical and genetic advantages.

This study is a pioneering investigation evaluating the usability of DNA obtained from human nails, especially mitochondrial DNA (mtDNA), as a biomarker. The research involved isolating DNA from challenging biological samples such as nails, demonstrating that mtDNA is more robust, stable, and suitable for amplification compared to nuclear DNA. Due to its high copy number per cell, mtDNA serves as a reliable genetic source, particularly in degraded or limited samples. The study showed that long mtDNA segments (over 9 kb) could be successfully amplified, and high consistency was observed both between individuals and within the same individual. These findings indicate that mtDNA is not only a molecule carrying hereditary information but also an effective biomarker in forensic sciences for individual tracking, identification, and toxicological monitoring. The ability to obtain mtDNA from nails provides significant advantages in postmortem analyses, aged or degraded samples, and minimally invasive sampling methods (Park et al., 2012).

SNP ANALYSIS

DNA isolation from nail samples allows for the performance of SNP (Single Nucleotide Polymorphism) analysis. Nails are particularly resilient and resistant to degradation compared to blood or tissue samples, enabling reliable genetic information to be obtained through SNP analysis even from samples that have been stored for long periods or preserved under suboptimal conditions. SNP analysis facilitates the use of DNA extracted from nails for forensic purposes such as genetic identification, individual recognition, and lineage tracing. Additionally, nail samples offer practical advantages as they are non-invasive and easy to collect.

However, since the amount of DNA obtained from nails is generally limited, it is crucial to use highly sensitive methods capable of working with low DNA quantities. Therefore, SNP analysis is often supported by next-generation sequencing (NGS) or specialized genotyping techniques. In conclusion, performing SNP analysis on nail material in forensic cases is both technically feasible and a practical, reliable approach (Truong et al., 2015).

SCIENTIFIC PRINCIPLES OF COLLECTING NAIL AND FINGERNAIL MATERIALS

Proper evidence collection is crucial in forensic nail analysis, requiring attention to detail and strict adherence to standard protocols. As the integrity of the evidence directly affects its legal validity, collection must always be carried out in accordance with standards.

STANDARD PROCESS PROCEDURES

Nail evidence collection is usually done in three main ways: cutting, swabbing or scraping. For cutting, experts should carefully cut the specimens with sterilized metal nail clippers and package the specimens appropriately (Badiye et al., 2023).

In addition, it is essential that those performing the procedure wear gloves and change them regularly to minimize the risk of contamination (Kleypas and Badiye, 2023).

Each nail sample must be cleaned of external contaminants before analysis. This is usually done by washing with water, soap or organic solvents. Samples should be stored in paper envelopes in limited light and at room temperature to preserve the integrity of the evidence. To collect any potential cellular debris, nail clippings are cleaned by elution in sodium acetate at 56°C for one hour and then subjected to DNA extraction. Other sample types (nail scrapings, swabs and smears) are extracted directly. DNA isolation is initiated by lysis using Proteinase K, DTT and SDS, followed by organic extraction and then concentrated and purified using centricon 100. (Sagar,2021; FernándezRodríguez et al., 2003). In nail samples rich in keratin, the samples are pre-treated with Proteinase K before DNA isolation to facilitate the breakdown of keratin (Bengtsson et al., 2012).

TRANSPORTATION TO THE LABORATORY AND STORAGE

The chain of custody requires detailed documentation of evidence at each stage (transfer, analysis, disposition). Improper preservation of nail samples in forensic science negatively affects the quality of the evidence and the analysis results. Firstly, nail samples should not be stored in moist or wet environments because moisture promotes the growth of microorganisms and leads to DNA degradation. Storing them in plastic bags for extended periods is also unsuitable, as plastic traps moisture and encourages the development of mold and bacteria. Therefore, nail samples should be preserved in breathable paper envelopes or special perforated containers (see Figure 2).

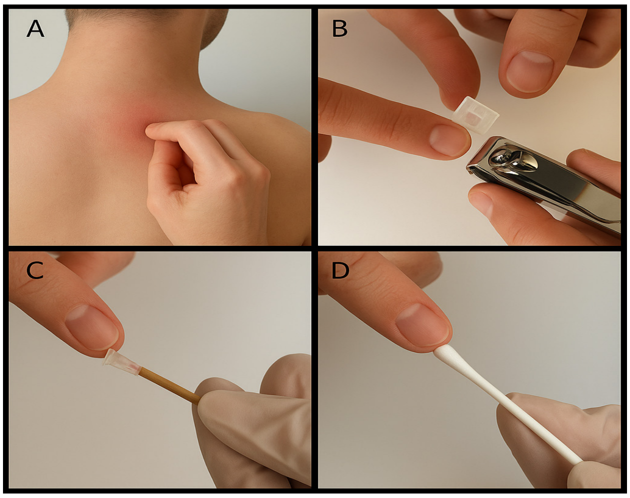

Figure 2. Collection of biological material from under the fingernail.

(A) DNA sampling from the nail

Methods used in the collection of samples: (B) Nail clipping, (C) Toothpick swab, and (D) Commercial swab.

Additionally, exposure to high temperatures and direct sunlight accelerates DNA degradation and damages the biological material, so they should be kept in a cool, dry, and dark environment. Contact with chemical substances should also be avoided, as chemicals such as alcohol and disinfectants can contaminate the samples. To prevent contamination, samples should not be handled without gloves and should not come into contact with other biological materials. Finally, nail samples should not be stored for long periods without proper conditions and should be delivered to the laboratory as soon as possible, because prolonged storage decreases DNA quality and reduces the reliability of the analyses. The storage condition of the nails should be in a sterile tube. The sample can then be stored for one week (Hamzaoglu and Yavuz, 2024). It has been demonstrated that DNA from nails remains suitable for successful SNP detection analyses even after cut nail fragments have been stored at room temperature for over 20 years (Van Breda et al., 2007).

In this process, the following information should be recorded for each evidence transfer:

Date and time, processors names and signatures, contact details and official addresses, unique instance identifiers, authorization details and transportation methods (see Figure 3). The number of transfers should be kept to a minimum and samples should be stored in secure areas accessible only by authorized persons. In addition, tampering with evidence should be prevented (Sagar,2021).

Figure 3. Nail Sample Collection Kit

STUDIES ON FINGERNAIL AND UNDER NAIL MATERIALS

DNA material under the nails has been examined in forensic laboratories for many years. Over time, various studies have been conducted on how long foreign biological materials can be preserved under the nail and how many days after the incident nail samples can still be taken (as shown in Table 1). In addition, different theories and techniques have been developed regarding the method of collecting nail samples and the transfer of the samples taken (Dogan et al., 2020).

However, there is no general consensus on which of these methods is the most effective or most efficient.

In forensic cases, nail samples of the victim are taken at autopsy or by medical personnel under appropriate conditions. The method of transferring samples to the laboratory may affect the results of DNA analysis.

Table 1. Studies on Fingernail and Under Nails Materials (Chronological Order)

Study No	Author & Year	Aim	Material / Sample	Method / Techniques	Key Findings	Conclusion / Recommendation
1	Cook and Dixon, 2007	Examine transfer of biological material under nails and mixed DNA profiles	Subungual (under nail) material	Qiagen column-based DNA extraction, STR profiling with AmpFISTR SGM Plus kit	Mixed DNA profiles detected in 13 samples; only 6 reportable	Subungual samples require careful interpretation due to mixed DNA
2	Matte et al., 2012	Investigate foreign DNA transfer under nails during routine activities	Nail scrapings from 14 lab staff	Nail scrapings collected by cutting scraper tips and damp swabs	Mixed DNA profile in 1 of 14 scraper-cut samples; none in swab samples	Swabbing less likely to detect mixed DNA; cutting scraper more sensitive
3	Preuner et al., 2014	Evaluate DNA isolation from nails and its quality and usability in genetic analyses (PCR, NGS, HLA typing)	Human nails	Prepfiler DNA extraction kit, PCR, NGS, high-resolution HLA analysis	High PCR amplification success (60-93%), reliable results in NGS and HLA analyses	Nail DNA is non-invasive, practical, and suitable for genetic analyses
4	Hebda et al., 2014	Investigate transfer of biological material between nails stored together	Bloody and clean nail samples in same envelope	Storage for 5 days in envelope, DNA quantification	No transfer detected, but DNA quantity halved	Nails should be stored in separate tubes to prevent DNA loss
5	Bozzo et al., 2015	Study mixed DNA profiles in nail samples collected by different methods during autopsy	164 nail samples during autopsy	DNA extraction: direct, cutting, swab methods; STR analysis	Victim DNA in all direct extractions; mixed profiles in some cutting and swab samples	Direct extraction best for pure DNA; swab and cutting methods may produce mixed profiles
6	Truong et al., 2015	Compare DNA isolation from nails to blood for SNP genotyping and null allele detection	Human nails and blood samples	PCR, Whole Genome Amplification (OmniPlex and MDA compared)	Over 96% SNP concordance; OmniPlex method showed superior performance	Nails provide high-quality DNA comparable to blood; OmniPlex WGA method recommended
7	Iuvaro et al., 2018	Simulate attacks to assess male DNA transfer under nails and persistence over time	160 nail samples from female volunteers scratching males	Real-time PCR, Y-STR analysis	High male DNA yields immediately after scratching; significant decrease after 5 hours	Nail samples collected shortly after incident more reliable for forensic analysis
8	Inkret et al., 2020	Optimize protocol for nail DNA isolation from severely decomposed human remains	Decomposed/ skeletal human nails	DTT-containing $TN_{(}Ca_{)}$ buffer, Qiagen EZ1 automated DNA extraction, PowerQuant qPCR, STR profiling	High-quality DNA obtained; PCR inhibitors detected	Optimized method allows reliable forensic identification from degraded nails
9	Yuksel et al., 2021	Compare undernail biological material collection methods	12 volunteer pairs: men buccal swabs, women undernail samples	Nail clipping, swabbing, cotton-wrapped fine-tipped toothpick swab	Nail clipping gave highest DNA yield but female DNA suppressed male alleles; cotton toothpick best for STR profiles	Cotton-wrapped fine-tipped toothpick swab recommended for reliable undernail DNA sampling
10	Ochiai et al., 2022	Evaluate effectiveness of new pre-processing method HONMA for nail DNA extraction	Human nails	HONMA (Horizontal Nail Mashing), PCR, STR profiling	Increased DNA yield, reduced processing time, decreased PCR inhibitors	HONMA method is practical and effective, yielding better forensic analysis results
11	Fokias et al., 2023	Perform forensic age estimation using DNA methylation analysis from nail tissue	Nails from 108 living and 5 deceased individuals	Sodium bisulfite conversion, pyrosequencing, CpG methylation analysis, OLS regression models	Mean error 5.48-9.36 years; accurate predictions even in deceased samples	Nail tissue is reliable and environmentally resilient alternative for forensic age estimation
12	Yuksel et al., 2024	Compare nail biological material collection methods	Nail clipping, thick and thin cotton swabs	STR analysis	Nail clipping collects more material and yields better DNA analysis success	Prefer nail clipping in critical cases for better identification accuracy

13	Della Rocca et al., 2024	To obtain high-quality DNA from nails of bodies submerged in seawater and determine paternal lineage by Y-STR	Nails of 5 bodies decomposed in seawater	Y-STR analysis, comparison with INTERPOL references	Y-STR analysis of nail DNA is reliable for paternal lineage identification	Nail Y-STR analysis effective for paternal lineage, useful in decomposed bodies
14	Sujirachato et al., 2024	Evaluate spin column-based method efficiency for nail DNA isolation	Nail samples from 30 healthy individuals	GeneAll® Exgene™ Cell SV Mini Kit, NanoDrop, PCR (HGH gene)	High purity (96.7%), average 0.816 µg DNA, successful HGH gene amplification	Spin column method is simple, reliable, and yields high-quality nail DNA
15	Damour et al., 2025	Evaluate duration male DNA detectable on female nails after contact and background DNA presence	Simulated contact samples	Y-STR profiling	Male DNA detected up to 6 hours; rapid decrease in 3 hours; background DNA remains up to 24 hours	Prompt sample collection advised; consider background DNA context in interpretation
16	Hulst et al., 2025	Create comprehensive forensic biological profiles from a single tooth and nail sample	7 postmortem cases: nail, tooth, blood samples	DNA analysis, isotope analyses (Sr, Pb, O, C), toxicology, C14 dating	77% success in nail analyses, 80% in tooth; nail DNA and toxicology analyses more successful	Multidisciplinary approach allows broad forensic info from few samples; nails are effective

In the study Y-STR analysis was performed on nail samples taken from five cadavers that had deteriorated in seawater for a long time. The aim of the study was to obtain high quality DNA from decomposed cadavers using nail material and to make identification with this DNA. The study aimed to determine the paternal lineage of the cadavers using Y-STR profiles obtained from the fingernails. The genetic profiles obtained were validated against references provided by INTERPOL and the results showed that fingernails can be used as a reliable source of DNA in such cases. The study highlights that fingernails offer an effective source for obtaining DNA from decomposed cadavers and that Y-STR analysis is a powerful method for paternal ancestry identification. In conclusion, this research reveals the potential and wider use of fingernails in forensic cases (Della Rocca et al., 2024). For this reason, it is more advantageous to perform Y-STR analysis by going from the male profile to determine ancestral lineage.

The usability and quality of DNA obtained from fingernails for genetic analyses were thoroughly evaluated. High-quality DNA was successfully isolated from fingernails using the Prepfiler Forensic DNA Extraction kit, and these DNA samples demonstrated high amplification success rates with PCR across genetic sequences of varying lengths. Amplification success rates were 93% for short (<300 bp), 90% for medium (>400 bp), and 60% for long (>2 kb) sequences. Additionally, the DNA isolated from fingernails was found suitable for next-generation sequencing (NGS) methods and provided reliable results in complex genetic analyses such as high-resolution HLA typing. These findings indicate that fingernails can serve as a non-invasive source of biological material, especially in cases where sample availability is limited, and can be safely used in forensic and genetic analyses. This method offers a practical alternative that enhances patient comfort in situations where blood or tissue samples are difficult to obtain. The isolated DNA was properly prepared for NGS by constructing DNA libraries, during which adapters were ligated to DNA fragments and amplification was performed. Thanks to high-resolution HLA typing, it was demonstrated that fingernail DNA allows successful analysis even in genetically complex regions. In conclusion, NGS analyses performed on DNA obtained from fingernails were found successful both in quality and coverage, confirming its suitability for advanced genetic testing (Preuner et al., 2014). As seen from the study, the usability of DNA obtained from fingernails for genetic analyses is demonstrated in detail. High-quality DNA was isolated from fingernails using the Prepfiler Forensic DNA Extraction kit, and high amplification success rates were achieved across genetic sequences of varying lengths using the PCR method. Additionally, the isolated DNA was shown to be suitable for next-generation sequencing (NGS) techniques; DNA libraries were constructed, and adapter ligation and amplification processes were successfully carried out. It was also proven that fingernail DNA provides reliable results in complex genetic analyses such as high-resolution HLA typing. The success of the methods used indicates that fingernail samples serve as a non-invasive and practical alternative in forensic and clinical genetic analyses.

This study investigates whether human nail clippings can serve as a reliable biological source for DNA analysis. The researchers compared DNA isolated from nail samples with DNA obtained from matched blood samples to assess the success of SNP genotyping and null-allele detection. The results demonstrated over 96% concordance in SNP genotyping and 100% agreement in null-allele detection between the two sample types. Following DNA extraction, specific gene regions were amplified using polymerase chain reaction (PCR), and whole genome amplification (WGA) methods were employed for genotyping. Two different WGA techniques, OmniPlex and Multiple Displacement Amplification (MDA), were compared, with OmniPlex yielding superior performance in both SNP and null-allele genotyping. Overall, the findings suggest that nail clippings, as a non-invasive and practical biological sample, can provide DNA of sufficient quality for genetic studies, and that OmniPlex-based WGA enables high-accuracy genetic analysis from such material (Truong et al., 2015). This study demonstrates that nail clippings are a reliable and high-quality biological source for DNA analysis. DNA obtained from nails showed a high degree of concordance when compared to DNA from blood samples. Specific gene regions were amplified using PCR, and two different whole genome amplification methods were tested for genotyping, with the OmniPlex method yielding better results. In conclusion, nail samples are a non-invasive and practical option that can be used for accurate and reliable genetic analysis.

In the study nail samples were utilized to extract DNA from severely decomposed or partially skeletonized human remains. To effectively break down the tough keratin structure of the nail tissue, the isolation protocol was optimized by adding DTT (Dithiothreitol) to the TN(Ca) buffer, which is typically used for bone tissue isolation, and DNA was automatically extracted using the Qiagen EZ1 Investigator Kit. The extracted DNA was quantified in terms of quantity and quality using the PowerQuant real-time PCR system, which also allowed for the detection of any PCR inhibitors. High-quality DNA samples were then subjected to STR profiling using the NGM STR kits, which are considered standard in forensic identification. The results demonstrated that the optimized method successfully yielded reliable, high-quality DNA from nail samples, indicating that this material can serve as an effective alternative for forensic identification in cases involving advanced decomposition (Inkret et al., 2020). This study shows that nail samples are a reliable source of DNA, especially for severely decomposed or partially skeletonized human remains. The isolation protocol was optimized to break down the tough keratin structure by using DTT, allowing efficient DNA extraction. The quality and quantity of the extracted DNA were thoroughly evaluated, and STR profiling demonstrated that the DNA could be effectively used for forensic identification. This indicates that nail samples provide an effective and reliable alternative for DNA analysis in challenging forensic cases.

In the traditional approach to extracting DNA from nails, the dissolution process typically requires about half a day. This study focuses on enhancing the efficiency of DNA extraction from nail samples by assessing a novel preprocessing technique known as Horizontal Nail Mashing (HONMA). This method involves mechanically compressing the nail to produce a thinner, more uniform sample, which facilitates improved DNA release. Compared to traditional digestion methods, HONMA significantly reduces processing time while increasing DNA yield. Additionally, the method lowers the likelihood of PCR inhibitors interfering with downstream genetic analyses, resulting in more consistent and accurate STR profiles. These findings suggest that HONMA offers a practical and effective approach for forensic DNA analysis from nail material, making it a valuable tool in forensic science (Ochiai et al., 2022). This study reveals the development of a new technique called Horizontal Nail Mashing (HONMA), which accelerates and improves the efficiency of DNA extraction from nails compared to traditional methods. HONMA mechanically compresses the nail to create a thinner and more uniform sample, allowing DNA to be released more easily. As a result, processing time is reduced, DNA yield increases, and the effect of PCR inhibitors is minimized. Consequently, this method provides more consistent and accurate results in forensic DNA analyses and offers a practical solution.

In this study, the potential of human nail tissue as an alternative biological sample for forensic age estimation was investigated by analyzing DNA methylation patterns. Due to its keratinized structure, nail tissue is highly resistant to environmental degradation, making it a valuable source in forensic contexts where conventional biological materials such as blood, saliva, or hair may be unavailable or compromised. A total of 108 nail samples (both fingernails and toenails) were collected from living individuals ranging in age from 0 to 96 years. Additionally, postmortem samples were obtained from five deceased individuals to assess the applicability of the method to forensic casework involving decomposed remains. Genomic DNA was extracted from the nail samples and subjected to sodium bisulfite conversion, a chemical treatment that distinguishes methylated from unmethylated cytosines. This conversion was followed by pyrosequencing, a quantitative method used to analyze DNA methylation levels at selected CpG sites. The study focused on 15 CpG sites located within four gene regions previously validated in age estimation models: ASPA, EDARADD, PDE4C, and ELOVL2. The methylation data were analyzed using ordinary least squares (OLS) regression models, constructed both as limb-specific (separately for fingernails and toenails) and combined models using data from all samples. The prediction accuracy of these models, measured by Mean Absolute Error (MAE), ranged from 5.48 to 9.36 years, depending on the source and type of nail sample. These results indicate that methylation signatures in nail DNA provide a reliable basis for chronological age estimation. Furthermore, the models were successfully applied to the postmortem nail samples, confirming that age prediction based on methylation markers remains feasible even after death. This finding supports the potential use of nail tissue in forensic investigations, especially in cases involving highly degraded remains. Overall, the study introduces a novel and practical approach to forensic age prediction and expands the range of viable biological materials that can be utilized in the field of forensic epigenetics (Fokias et al., 2023). This study shows that nail tissue can be used as a reliable biological sample for age estimation through DNA methylation analysis. Due to its resistance to environmental degradation, nail tissue is especially valuable in cases involving decomposed remains. DNA was extracted from nail samples collected from 108 living individuals and 5 deceased individuals. Methylation analyses were performed, and age prediction models were developed. These models demonstrated high accuracy. As a result, it was concluded that age estimation is possible even after death using methylation data from nail tissue.

In other research, investigated the effectiveness of a spin column-based nucleic acid purification technique for extracting DNA from nail samples. DNA was isolated from nails collected from 30 healthy individuals using the GeneAll® Exgene™ Cell SV Mini Kit. The quantity and purity of the extracted DNA were assessed via NanoDrop spectrophotometry, while DNA integrity was verified through PCR amplification of the human growth hormone (HGH) gene. The average DNA yield was measured at 0.816 µg, with an average concentration of 27.2 ng/µL. Notably, 96.7% of samples demonstrated high purity levels (A260/A280 ratio ≥ 1.80). Successful amplification of a 434 bp HGH fragment confirmed the DNA quality. These findings suggest that the spin column method is a straightforward and reliable approach for obtaining high-quality DNA from nails, highlighting the potential of nail samples as a valuable resource in forensic investigations (Sujirachato et al., 2024).

In another study assessed the feasibility of generating a comprehensive forensic biological profile using a single tooth and nail sample. Postmortem samples of toenails, teeth, and blood from seven cases were analyzed following a multidisciplinary protocol. Various techniques, including DNA analysis, isotope analyses (Sr, Pb, O, C), toxicological assessments, and carbon-14 (14C) measurements, were employed. Among 56 analyses conducted on tooth samples, an 80% success rate was achieved, while 77% of the 35 analyses on nail samples were successful. DNA, toxicology, and 14C analyses performed better in nail samples compared to teeth, whereas isotope analyses yielded more reliable results in tooth specimens. The study enabled the determination of crucial forensic information such as birth and death dates, age, sex, geographic residency throughout life, and exposure to different drugs. In conclusion, this multidisciplinary approach allows for the extraction of valuable and comprehensive forensic data from a limited number of biological samples, offering an effective protocol that reduces sample requirements in forensic investigations (Hulst et al., 2025).

WORK ON THE TRANSFER OF MATERIALS

Hebda et al. have shown that putting nails in the same envelope can lead to the transfer of biological material. In their experiments, they kept bloody and clean nail samples in the same envelope for 5 days, finding that there was no transfer, but the amount of DNA was halved. They suggested that the nails be carried in tubes to prevent DNA loss (Hebda et al., 2014).

OBSERVATION OF MIXED DNA PROFILES IN MATERIALS

In the study, 164 nail samples taken during autopsy were subjected to DNA analysis by three different methods. While the DNA of the victim was detected in all of the samples that were directly extracted, mixed DNA profiles were obtained in some of the samples taken by cutting and swab methods. While only the victim's DNA was found in 75% of the samples examined, foreign DNA was detected at a reportable level in 10%. From this study, the team deduced the following, while detecting the victim's DNA in all of the samples taken by direct extraction method; He stated that mixed DNA profiles were found in some of the samples taken by swab and cutting methods (Bozzo et al., 2015). Although it is accepted that biological material can be passed from one person to another during routine activities, some studies indicate that this material cannot produce mixed profiles at a reportable level (Nurite et al., 2011; Dowlan et al., 2010; Cline et al., 2003).

In mixed DNA profiles, the presence of more than one allele at some loci is the first indicator. Peaks can be similar in size, depending on the amount of DNA of individuals, or one can dominate over the other. In this case, the dominant profile is called major (major) peaks, and the other is called minor (minor) peaks (Gill and Haned, 2013).

Analysis of mixed DNA profiles is challenging. For a peak to be considered minor, its height must be at least 10% of the major peak (Bille et al., 2019).

In some women's fingernails, although there were peaks in the autosomal DNA profile of only the sample owner, a complete DNA profile of a man was also found in the Y-STR analysis. This study makes it clear that extreme caution is required when examining mixed profiles in the analysis of nail samples (Malsom et al., 2009).

In a study, it was reported that the transfer of biological material under the nail was examined and mixed DNA profiles were detected in only 13 samples, only 6 of which were reportable. In the referenced study, DNA was extracted from subungual (under the fingernail) material and subsequently analyzed to generate DNA profiles. DNA isolation was performed using a column-based method with a commercially available Qiagen DNA extraction kit. The resulting DNA samples were then subjected to profiling using the AmpFISTR SGM Plus kit. This kit is based on Short Tandem Repeat (STR) analysis, a widely used technique in forensic genetics due to its high accuracy and reproducibility. The STR-based approach enabled reliable identification of individual-specific genetic variations, allowing for accurate comparative analysis of the DNA profiles obtained in the study. (Cook and Dixon, 2007).

In a study, conducted by Iuvaro et al. in 2018, attack situations were simulated with a controlled scenario in which female volunteers scratch male volunteers. A total of 160 nail samples were collected, of which 80 were analyzed as control (before scratching), 40 immediately after scratching and 40 5 hours later. The aim was to assess the transmission of male DNA under the nail and its persistence over time by real-time PCR and Y-STR analysis. The data showed that high yields of male DNA and good quality Y-STR profiles were obtained in samples collected immediately after scratching, but this yield and profile quality were significantly reduced after 5 hours. The results suggest that nail samples collected shortly after the incident are more reliable for forensic analysis (Iuvaro et al., 2018).

The study conducted by Damour et al. in 2025 evaluates how long male DNA can be detected on female fingernails after physical contact and the presence of background DNA. The findings show that DNA from a male individual's Y-STR profile can be detected up to 6 hours after simulations and that the proportion of DNA traces consistent with the suspect (POI) is high in samples immediately after the incident. However, this rate drops rapidly in the first 3 hours, and after 12 and 24 hours, these traces are not detected. Remarkably, 44% of the DNA profiles obtained after 24 hours matched the profiles detected before the incident. This suggests that background male DNA from daily activities or close contacts may remain under the fingernail. In conclusion, prompt collection of fingernail samples after the assault may facilitate the detection of offender DNA while minimizing the effect of background DNA. In addition, the study emphasizes that sub-source DNA findings should not be overly interpreted and the context of the incident should be taken into account in the evaluations (Damour et al., 2025).

STUDIES ON THE APPLICATION OF SWAB METHOD

In 2012, Matte et al. investigated the transfer of foreign DNA under the nail during routine activities. In the study, 14 staff members working in their laboratories were asked to scrape their nails with a wooden scraper, and a total of 28 samples were created by combining five scrapers for each hand. Half of the samples were analyzed by cutting the scraper ends and the other half were taken with a damp swab. As a result, a mixed DNA profile was detected in only one of the 14 samples in which the scraper tips were cut and examined, while the mixed profile could not be determined in the 14 samples taken by the swab method (Matte et al., 2012). In the project carried out by Yuksel et al. in 2021, an experimental scenario was created in line with the data obtained from 12 volunteer pairs and the methods of collecting undernail material were compared. While reference DNA samples were taken from men by buccal swab method, samples were collected from women by applying three different undernail material collection procedures. In this study, these three different procedures were compared in order to determine the most efficient sample collection method. The methods of collecting undernail material are as follows: cutting the nails and placing them in a tube, taking a swab from under the nail with a swab used in routine procedures, and finally, the sample was collected using a toothpick and a fine-tipped swab made of cotton. As a result of the STR analysis, the compatibility of these methods with the reference DNA sample was evaluated and the most effective method was tried to be determined. According to DNA quantity analysis, the highest amount of DNA was obtained from nail clippings. However, it has been observed that allele peaks of female DNA suppress allele peaks of male DNA in some STR loci. In DNA samples obtained using swabs, STR profiles could not be obtained in some pairs, while profiles mixed with female DNA were detected in some other samples. As a result of the study, it was determined that the most successful method in terms of creating an STR profile and reliably reporting the biological material taken from under the nail is the cotton-wrapped fine-tipped toothpick swab method (Yuksel et al., 2021).

Yuksel et al. in 2024, conducted a comparative study on nail biological material collection methods, which are critically important in forensic sciences. The study evaluated swabbing techniques using both thick and thin cotton swabs alongside nail clipping. Results demonstrated that nail clipping collected more material and achieved higher success in DNA analysis. Although cotton swab methods are practical, the amount of material collected is limited. The research emphasizes the vital importance of selecting the appropriate material collection method for accurate identification and evidence reliability, highlighting the need to optimize nail material collection procedures. Overall, in critical cases, preferring nail clipping can improve the accuracy of DNA analyses and enhance identification reliability. These findings provide valuable data for improving evidence collection practices in forensic sciences (Yuksel et al., 2024).

CONCLUSION AND RECOMMENDATIONS

Although nail samples are used in forensic genetic analysis in cases of murder, sexual abuse and suicide, the involvement of different experts in the process prevents the formation of a standard procedure. While the samples taken during the autopsy are examined in DNA laboratories, sampling and analysis methods have diversified over time, but no definitive study has been made on the most efficient method. It is important to prevent loss of evidence in the transfer of nail samples. Carrying them in the same envelope can lead to DNA cross-contamination. To avoid this, each nail must be sent to the laboratory in a separate tube. The researchers stated that undernail samples can best be taken by the "swab" method, but emphasized that a separate swab should be used for each nail (Hebda et al., 2014). Some experts have argued that this is disadvantageous in terms of time, workload and cost (Bozzo et al., 2015). Inserting the cut nails into the solution increases the DNA density of the victim, while collecting all swab samples in a single tube can complicate the DNA profile when there is more than one suspect (Ottens et al., 2015). The gender of the victim and suspect is an important factor when working with nail samples. If the victim is a woman and the suspect is a man, Y-STR analysis can play a critical role. In autosomal STR analysis, the dense DNA of the victim masks a small amount of DNA from the suspect, while Y-STR analysis can clearly reveal the DNA of the suspect (Iuvaro et al., 2018). Nail samples should be taken as soon as possible. Because DNA may be lost. The person may wash their hands or touch other places, making it difficult to reach the DNA we are looking for. Real-time PCR and Y-STR profiling were used to assess the migration and persistence of male DNA under female nails after scratching. Comparison of nail samples taken immediately after scratching and 5 hours later showed a significant decrease in DNA yield and a parallel decrease in Y-STR profile quality (Iuvaro et al., 2018). In conclusion, there is a need for further elaboration of experimental studies and investigations into storage conditions. With the advancement of time and technology, the development of new kits and methods is expected to enhance the feasibility of obtaining high-quality DNA.

References

1. Alford RL, Hammond HA, Coto I, Caskey CT. (1994). Rapid and efficient resolution of parentage by amplification of short tandem repeats. *Am J Hum Genet.*, 55:190-195.
2. Allen M., Engstrom A.S., Meyers S., Handt O., Saldeen T., Haeseler A., Paabo S., Gyllensten U. (1998), Mitochondrial DNA sequencing of shed hairs and saliva on robbery caps: sensitivity and matching probabilities, J Forensic Sci 43: 453– 464.
3. Badiye, A., Kapoor, N., & Menezes, R. G. (2023, February 13). Chain of custody. In StatPearls. StatPearls Publishing. Retrieved June 8, 2025, from https://www.ncbi.nlm.nih.gov/books/NBK553101/
4. Bengtsson, C. F., Olsen, M. E., Brandt, L. Ø., Bertelsen, M. F., Willerslev, E., Tobin, D. J., Wilson, A. S., & Gilbert, M. T. P. (2012). DNA from keratinous tissue. Part I: Hair and nail. *Annals of Anatomy - Anatomischer Anzeiger*, 194(1), 17-25.
5. Bille T., Weitz S., Buckleton J. S., Bright J. A. (2019). Interpreting a major component from a mixed DNA profile with an unknown number of minor contributors. *Forensic Sci Int Genet.*, 40, 150-159.
6. Bozzo W. R., Colussi A. G., Ortíz M. I., Laborde L., Pilili J. P., Carini G., et al. (2015). Analysis of DNA from fingernail samples in criminal cases. *Forensic Science International: Genetics Supplement Series*, 5, e601-2.
7. Brinkmann, B. (1992). The use of STRs in stain analysis. In:

Proceedings from the Third International Symposium on Human Identification. Promega Corporation, Madison, USA, 132: 357–373.
8. Budowle, B., van Daal, A. (2008). Forensically relevant SNP classes. *Biotechniques*, 44(5), 603-8, 610.
9. Butler JM. Short tandem repeat typing technologies used in human identity testing. Biotechniques. 2007;43:Sii–Sv.
10. Butler, J. M. (2011). Forensic DNA testing. *Cold Spring Harbor Protocols*, 2011(12), 1438–1450.
11. Cavuş Yonar, F., Sen Yılmaz, A., Cicek, F. (2024). Examination of trace evidence. F. Asıcıoğlu (Ed). In forensic sciences (pp. 62-79). Istanbul: IÜC University Publishing House.
12. Cerri N, Ricci U, Sani I, et al. Mixed stains from sexual assault cases: autosomal or Y-chromosome short tandem repeats? Croat Med J. 2003;44:289–292.
13. Cline, R. E., Laurent, N. M., & Foran, D. R. (2003). The fingernails of Mary Sullivan: developing reliable methods for selectively isolating endogenous and exogenous DNA from evidence. *J Forensic Sci.*, 48(2), 328-33.
14. Cook, O., & Dixon, L. (2007). The prevalence of mixed DNA profiles in fingernail samples taken from individuals in the general population. *Forensic Sci Int Genet.*, 1, 62-8.
15. Damour, G., Basset, P., Samie, L., & Salonu, D., (2025). Tracking male DNA transfer and survival under female victim fingernails: Insights from a 24-h scratch simulation. Forensic Science International: Genetics, Volume 78, 103280
16. De Bruin, K. G., Verheij, S. M., Veenhoven, M., vd. (2012). Comparison of stubbing and the double swab method for collecting offender epithelial material from a victim's skin. *Forensic Science International: Genetics*, 6(2), 219-223.
17. Della Rocca C, Chighine A, Piras G, Vecchio C, Mameli A. Nails as optimal source of DNA for molecular identification of 5 decomposed bodies recovered from seawater: from Y-ancestry to personal identification. Int J Legal Med. 2024 May;138(3):787-792.
18. Dowlman, E. A., Martin, N. C., Foy, M. J., vd. (2010). The prevalence of mixed DNA profiles on fingernail swabs. *Science & Justice*, 50(2), 64-71.
19. Ea D, Martin NC, Foy MJ, et al. The prevalence of mixed DNA profiles on fingernail swabs. Sci Justice. 2010;50:64–71.
20. Edwards, A., Civitello, A., Hammond, H., & Caskey, C. (1991). DNA Typing And Genetic Mapping With Trimeric And Tetrameric Tandem Repeats. *American Journal Of Human Genetics*, 49(4), 746.
21. FernándezRodríguez, A., Iturralde, M. J., Fernández de Simón, L., Capilla, J., & Sancho, M. (2003). Genetic analysis of fingernail debris: Application to forensic casework. *International Congress Series, 1239*, 921–924. Elsevier Science.
22. Fokias, K., Dierckx, L., Van de Voorde, W., & Bekaert, B. (2023). Age determination through DNA methylation patterns in fingernails and toenails. *Forensic Science International: Genetics*, *64*, 102846.
23. Giles R.E., Blanc H., Cann H.M., Wallace D.C. (1980) Maternal İnheritance Of Human Mitochondrial-DNA, Proceedings Of The National Academy Of Scince Of The United States Of America-Biological Scinces 77:6715-6719.
24. Gill, P., & Haned, H. (2013). A new methodological framework to interpret complex DNA profiles using likelihood ratios. *Forensic Sci Int Genet.*, 7(2), 251-263.
25. Goodwin W., Linacre A., Vanezis P. (1999), The use of mitochondrial DNA and short tandem repeat typing in the identification of air crash victims, Electrophoresis 20: 1707- 1711.
26. Hamzaoglu, N., Yavuz, M. F. (2024). Biological sampling in cases of sexual assault. G. Filoğlu & Ö. Bülbül (Eds). Forensic biology: In pursuit of justice with traces of nature II (pp. 24-29). Istanbul: IÜC University Publishing House.
27. Hebda, L. M., Doran, A. E., & Foran, D. R. (2014). Collecting and analyzing DNA evidence from fingernails: a comparative study. *J Forensic Sci.*, 59(5), 1343-1350.
28. Hulst, R. V. D., Gerretsen, R. R., Kootker, L. M., Palstra, S. W., Kal, A. J., Ammer, S., ... & Touw, D. J. (2025). A multidisciplinary approach to forensic biological profiling on a single tooth and nail sample. *International journal of legal medicine*, *139*(1), 361-374.
29. Hopwood A.J., Mannucci A., Sullivan K.M. (1996), DNA typing from human faeces, International Journal of Legal Medicine 108: 237-243.
30. Iuvaro, A., Bini, C., Dilloo, S., Sarno, S., & Pelotti, S. (2018). Male DNA under female fingernails after scratching: transfer and persistence evaluation by RT-PCR analysis and Y-STR typing. *Int J Legal Med.*, 132(6), 1603-1609.
31. Inkret, J., Podovšovnik, E., Zupanc, T. et al. Fingernails as primary sample type for molecular genetic identification of highly decomposed human remains. Int J Legal Med 134, 1629–1638 (2020). https://doi.org/10.1007/s00414-020-02289-x
32. Karadayı S, Arasoglu T, Karadayı B, et al. Assessment of the exclusion potential of suspects by using microbial signature in sexual assault cases: a scenario-based experimental study. Forensic Sci Int. 2021;325:110886.
33. Kayser M. Forensic use of Y-chromosome DNA: a general overview. Hum Genet. 2017 May;136(5):621-635. doi: 10.1007/s00439-017-1776-9.
34. Kleypas, D. A., & Badiye, A. (2023, May 8). *Evidence collection*. In StatPearls. StatPearls Publishing. Retrieved June 8, 2025, from https://www.ncbi.nlm.nih.gov/books/NBK539904/
35. Malsom, S., Flanagan, N., McAlister, C., & Dixon, L. (2009). The prevalence of mixed DNA profiles in fingernail samples taken from couples who cohabit using autosomal and Y-STRs. *Forensic Sci Int Genet.*, 3(2), 57-62.
36. Matte, M., Williams, L., Frappier, R., & Newman, J. (2012). Prevalence and persistence of foreign DNA beneath fingernails. *Forensic Sci Int Genet.*, 6(2), 236-243.
37. Melton T. ve Nelson K. (2001), Forensic mitochondrial DNA analysis: Two years of commercial casework experience in the United States, Croat Med J. 42: 298-303.
38. Newton, M. (2013). The forensic aspects of sexual violence. *Best Practice & Research Clinical Obstetrics & Gynaecology*, 27(1), 77-90.
39. Nurit, B., Anat, G., Michal, S., Lilach, F., & Maya, F. (2011). Evaluating the prevalence of DNA mixtures found in fingernail samples from victims and suspects in homicide cases. *Forensic Sci Int Genet.*, 5(5), 532-537.
40. Ochiai, E., Asogawa, M., Irie, W., Sasaki, C., Nakamaru, N., Sakamoto, M., ... & Satoh, F. (2022). Examination of pretreatment methods for DNA extraction from nails. *Forensic Science International: Genetics Supplement Series*, *8*, 110-111.
41. Ottens, R., Taylor, D., & Linacre, A. (2015). DNA profiles from fingernails using direct PCR. *Forensic Sci Med Pathol.*, 11(1), 99-103.
42. Park, J., Liang, D., Kim, J. W., Luo, Y., Huang, T., Kim, S. Y., & Chang, S. S. (2012). Nail DNA and possible biomarkers: a pilot study. *Journal of Preventive Medicine and Public Health*, *45*(4), 235.
43. Pereira R., Gomes I., Amorim A., Gusmão L. (2007) Genetic diversity of 10 X chromosome STRs in northern Portugal. Int. J. Legal Med. 121: 192–197
44. Piccinini A. A 5-year study on DNA recovered from fingernail clippings in homicide cases in Milan. In: Brinkmann B, Carracedo A, editor. International Congress Series. Amsterdam (the Netherlands): Elsevier; 2003. p. 929–932.
45. Preuner, S., Danzer, M., Pröll, J., Pötschger, U., Lawitschka, A., Gabriel, C., & Lion, T. (2014). High-quality DNA from fingernails for genetic analysis. Journal of Molecular Diagnostics, 16 (4), 459-466.
46. Prinz M, Boll K, Baum H, Shaler B. Multiplexing of Y chromosome specific STRs and performance for mixed samples. Forensic Sci Int. 1997;14;85(3):209–18.
47. Robin E.D., Wong R. (1988), Mitochondrial DNA molecules and virtual number of mitochondria per cell in Mammalian cells, J Cell Physiol 136 : 507-513

48. Roux, C., Talbot-Wright, B., Robertson, J., Crispino, F., & Ribaux, O. (2015). The end of the (forensic science) world as we know it? The example of trace evidence. *Philosophical Transactions of the Royal Society B: Biological Sciences*, 370(1674), 20140260.
49. Sagar, G. (2021). Nail as Evidence in Forensic Toxicology, (100-101).
50. Shimamoto, G. G., Terra, J., & Bueno, M. I. M. S. (2013). Use of Portable X-ray Fluorescence to Discriminate Brands of Nail Polishes: a Potential Forensic Tool. *Journal of the Brazilian Chemical Society*.
51. Sujirachato, K., Wongyanin, P., Ramadjai, P., Ladsuk, A., Pokkasap, K., & Worasuwannarak, W. (2024). Study of the DNA Extraction from the Nail by Spin Column-based Nucleic Acid Purification. *Journal of Forensic Science and Medicine*, *10*(3), 191-195.
52. Steighner R.J., Holland M. (1998), Amplification and sequencing of mitochondrial DNA in forensic casework, Methods Mol Biol 98:213–223.
53. Szibor R., Krawzak M., Hering S., Edelmann J., Kuhlisch E., Krause D. (2003) Use of XLinked markers for Forensic purposes. International Journal of Legal Medicine, 117: 67–74.
54. Szibor R. (2007). The X-chromosome in forensic science: past, present and future, Molecular Forensics (R. Rapley, D. Whitehouse, Eds), pp. 103–126, John Wiley & Sons, Ltd
55. Truong, L., Park, H. L., Chang, S. S., Ziogas, A., Neuhausen, S. L., Wang, S. S., ... & Anton-Culver, H. (2015). Human nail clippings as a source of DNA for genetic studies. *Open journal of epidemiology*, *5*(1), 41.
56. Van Breda, S. G., Hogervorst, J. G., Schouten, L. J., Knaapen, A. M., van Delft, J. H., Goldbohm, R. A., ... & van den Brandt, P. A. (2007). Toenails: an easily accessible and long-term stable source of DNA for genetic analyses in large-scale epidemiological studies. *Clinical chemistry*, *53*(6), 1168-1170.
57. Watherston, J., McNevin, D., Gahan, M. E. E., Bruce, D., & Ward, J. (2018). Current and emerging tools for the recovery of genetic information from post mortem samples: New directions for disaster victim identification. *Forensic Science International: Genetics*, 37(March), 270-282.
58. Wilson M.R., Polanskey D., Butler J., DiZinno J.A., Replogle J., Budowle B. (1995), Extraction, PCR amplification and sequencing of mitochondrial DNA from human hair shafts, Biotechniques 18:662–669.
59. Wond, J. H. (2008). The Value of DNA Material Recovered from Crime Scenes. *J Forensic Sci.*, 53(4), 797-801.
60. Yuksel, E., Ozbek, T., & Karadayı, B. (2021). A comparative study on the collection and analysis of DNA evidence obtained from subungual material. 4th INTERNATIONAL HEALTH SCIENCES AND INNOVATION CONGRESS (pp. 672-680). Baku, Azerbaijan.
61. Yuksel, E., Karadayı, S., Ozbek, T., & Karadayı, B. (2024). A comparative experimental study on the collection and analysis of DNA samples from under fingernail material. *Forensic Sciences Research*, owae025.

HİTİT JOURNAL OF SCIENCE

e-ISSN: 3061-9629
Volume: 2 • Number: 2
July 2025

Vehicle Paint as Trace Evidence: Spectroscopic and Microscopic Characterization for Forensic Identification

Züleyha Katrancı Kaynak[1] | Ebru Gökmeşe[2,*] | Faruk Gökmeşe[2]

[1]Hitit University, Graduate Education Institute Department of Forensic Sciences, 19030, Çorum, Türkiye.
[2]Hitit University, Faculty of Engineering and Natural Sciences Department, 19030, Çorum, Türkiye.

Corresponding Author

Ebru GÖKMEŞE

E-mail: ebrugokmese@hitit.edu.tr Phone: +90 364 227 7000
RORID: ror.org/01x8m3269

Article Information

Article Type: Research Article
Doi: -
Received: 30.05.2025
Accepted: 10.07.2025
Published: 31.07.2025

Cite As

Kaynak ZK., Gökmeşe E., Gökmeşe F. Vehicle Paint as Trace Evidence: Spectroscopic and Microscopic Characterization for Forensic Identification. Hitit journal of Science. 2025;2(2):54-60.

Peer Review: Evaluated by independent reviewers working in at least two different institutions appointed by the field editor.
Ethical Statement: Not available.
Plagiarism Checks: Yes - iThenticate
Conflict of Interest: Authors approve that to the best of their knowledge, there is not any conflict of interest or common interest with an institution/organization or a person that may affect the review process of the paper.

CRedit Author Statement
Züleyha Katrancı Kaynak: Design of the study, Conceptualization, Writing-original draft, Editing, Supervision.
Ebru Gökmeşe: Design of the study, Conceptualization, Writing-original draft, Editing, Supervision.
Faruk Gökmeşe: Design of the study, Conceptualization, Writing-original draft, Editing, Supervision.

Vehicle Paint as Trace Evidence: Spectroscopic and Microscopic Characterization for Forensic Identification

Züleyha Katrancı Kaynak[1] | Ebru Gökmeşe[2,*] | Faruk Gökmeşe[2]
[1]Hitit University, Graduate Education Institute Department of Forensic Sciences, 19030, Çorum, Türkiye.
[2]Hitit University, Faculty of Engineering and Natural Sciences Department, 19030, Çorum, Türkiye.

Abstract
Vehicle paint is a common trace evidence in crime scene investigations of car accidents. The importance of car paints in terms of Forensic Sciences is highlighted by the transfer of paint samples from one car to another in car accidents, theft, or hit-and-run cases. The paint is considered evidence in all cases where vehicle paint is found as residue. Analyzes are performed with FT-IR, Raman, Pyr-GC/MS, and SEM/EDX. With the analysis methods, the basic characteristics of the paints on the vehicles involved in the incident can be determined. In this study, paint samples of five vehicles obtained from the auto industry in Çorum were pulverized and analyzed using FT-IR Spectroscopy and SEM/EDX methods. As a result of the analysis, it was observed that vehicles with different brands, models, and production years gave different results. SEM images of five vehicle paints provided information about surface topography. SEM results show that the paint samples have rough, cracked, and heterogeneous surface morphology. The analysis information for each vehicle varies, proving the importance of vehicle trace evidence.
The vehicles involved in the crime can be identified even without eyewitnesses or camera footage.
There is a need to create a vehicle database in our country. This study aims to contribute to the tool database library that can be used in forensic sciences in our country in the future.

Keywords: Vehicle Paint, Forensic Science, FT-IR, SEM/EDX, Trace Evidence

INTRODUCTION
Paints, or surface coatings, as they are technically called, are ubiquitous in daily life. They are applied to many surfaces, such as wood, paper, metal, and plastic, to increase the properties and durability of products [1].

There are no strict rules for the application of architectural paint, and situations where architectural paint is applied, often encountered in judicial cases, can be done by amateurs. On the other hand, vehicle paint applications are quite technical processes and are usually carried out by professionals [2]. Paint transfer, which is most common in automobile accidents, is a good example of material transfer that occurs when two objects come into contact [3]. In hit-and-run cases, a mutual paint change usually occurs between the offender's vehicle and the victim's vehicle involved in the collision.

Watercolors are a potential source of trace evidence in crime scene investigations. Due to their water-based nature, watercolor stains can easily contaminate the surfaces they come into contact with, and in this respect, they can carry other types of evidence. Watercolors can be essential, especially in detecting microscopic traces such as hair strands, cartilage pieces, and fibers. In addition, it is possible to detect individual-specific biometric traces such as fingerprints, palm prints, or ear prints on the watercolor layer. Such traces can make significant contributions both to the identification of the perpetrator and to establishing his connection with the incident [4].

Paint shavings and paint transfer are two types of evidence frequently used in forensic material analysis. Especially after traffic accidents, paint transfer between colliding vehicles contributes to illuminating the incident by providing information about the contact direction, impact intensity, and contacting surfaces. These analyses are essential in identifying the perpetrator's vehicle or the parties involved in the accident. In incidents such as theft, paint traces on the tools used by the perpetrator at the scene help establish a connection between the suspect and the crime scene. Paint layers transferred from door, window, or vehicle surfaces onto the tool can be analyzed with microscopic and spectroscopic techniques to reveal unique structural features [5]. For forensic analysis of multilayered paint chips of hit-and-run cars, composition analysis, including trace chemical components in multilayered paint chips, is crucial for identifying the getaway car. Depending on the car manufacturer and year of production, the number of layers, painting process, and paints used are specific to the car types, color, and surface protection. [6].

The most crucial element that makes the paint attractive is its color. Different types and amounts of minerals are used in paint formulas. Pigments are one of the cornerstones of paint, in the form of small particles that are insoluble in a solvent or a binder. Ordinary paint is a mixture of pigment particles, polymers, polyelectrolytes, and surfactants [7]. There are differences in brightness, chemical stability, cost, and durability between organic and inorganic pigments. Organic pigments contain carbon, while inorganic pigments do not contain carbon. Organic pigments such as azo, diazo, polycyclic, phthalocyanine, and quinacridone contain carbon, while inorganic pigments do not contain carbon (i.e., titanium dioxide, iron oxide and chromium oxide are inorganic pigments). [8]. Copper phthalocyanine blue and titanium dioxide are very common pigments used in paints. Most pigments used in paint produce color by selective absorption of specific wavelengths of visible light [9].

Paint chips and stains are left as physical evidence at hit-and-runs, crime scenes, and accidents that can be transferred from one vehicle to another or from one vehicle to the person hit. Before a paint sample is taken, a photograph is taken of the area containing the sample without disturbing the evidence. Crime scene investigators then collect the paint sample by carefully scraping or peeling it from the surface where it was found. Therefore, the investigating officer must be competent and effective in collecting paint evidence and be aware of paint's importance as physical evidence [10].

Paint chips taken during the paint collection process should contain all paint layers, if possible. While the collected physical evidence (glass containing paint samples, headlights, etc.) is sent to the laboratory with the help of plastic bags or glass bottles, if there are paint chips on the clothes, they are wrapped in clean paper and sent. Dry paint chips brought to the laboratory from the scene are subjected to a series of processes for analysis. The choice of method used depends on the product quantity and condition. The paint chip to be analyzed is evaluated visually and macroscopically. Suppose the sample is a paint chip as a result of macroscopic examination. In that case, the examination is continued with the help of a microscope, and the number and order of layers of the paint sample are determined. If there is a reference paint sample, the comparison is made. If a physical match is made, a report is kept. If there is no physical match, the sample is evaluated for the analytical approach. A sample suitable for the method to be used is prepared. The analyst applies solvent tests to the paint chip to see if the paint reacts by swelling, curling, softening, or other ways.

Significant diversity was found from primary surface coats using FT-IR microspectroscopy to characterize and evaluate the chemical diversity of paint samples from 75 vehicles representing a range of automobile manufacturers. Information such as manufacturing country, manufacturing facility, and vehicle production year were obtained in the classification made using principal component analysis. Obtaining this information from the analysis of interrogated automotive paint samples found at a crime scene or on the victim's clothing has been shown to assist in developing avenues of investigation [11]. The paint sample can be analyzed by taking a thin section with the help of a microtome or by pulverizing it. FT-IR spectroscopy, SEM, PC/GC-MS, and Raman spectroscopy can be used to analyze the paint chip instrumentally. Two analysis methods must give parallel results for the paint sample to be presented to the court as evidence. Since automotive paint parts are essential in forensic science, procedures have been defined to analyze vehicle paint samples. A new methodology is proposed to automate visual analysis using image acquisition. Based on the microscopic image of a paint sample, color and texture information was obtained and compared with paints with the same properties for the paint database. Experiments have shown that the proposed methodology is valid, and the same type of pigment is present both in the paint samples and the database [12].

PDQ (Paint data query) is an international automotive paint database used by forensic scientists at 102 forensic laboratories in 24 countries (including 58 forensic laboratories in 32 states in the United States) to help identify possible suspect vehicles with paint evidence left at crime scenes. The binder and pigment formulations in each layer of the paint create unique combinations that determine the vehicle's likely make, model, and year range. Each paint layer is separated and placed between two diamonds for infrared analysis when analyzing an automotive paint sample. Each component has a characteristic fingerprint known as the infrared spectrum. From there, it includes complete source information for each sample, color descriptions of each paint, the chemical composition of each layer, and layer sequence information, including images of each spectrum [13].

Comparative analysis of paint traces can identify pigment transfer between vehicles during a crash, objects such as crowbars or screwdrivers used to break windows, cars or safes, or the source of spray paint. This allows for tracking vehicle types in hit-and-run accidents and catching thieves who unknowingly transfer paint from the robbery area to any tools they use [14].

To distinguish different pigments with similar tones, microscopic traces of the samples must be taken with high chemical specificity and analyzed non-destructively and comparatively. Raman microscopy meets both criteria due to its high spectral resolution, spatial resolution in the submicron range available, and no need for sample preparation [14].

Duarte et al.'s research examines studies on paint trace evidence published between 2010 and 2019. Information on paint layers, model validation, chemical characterization, and sample origins is available. In addition to FT-IR and Raman spectroscopies, they mentioned optical coherence tomography as an alternative. They also emphasized that chemometric techniques were used when analyzing the spectra [15].

Since auto paints of the same brand and color differ depending on the year of production in terms of chemical content, pigment type, layer structure, elemental content, and resin type, thanks to these differences, a year-based distinction can be made with forensic analysis. Different resin types, binder changes, and solvent bases emerge thanks to the determination of functional groups. Changes in pigment formulations over the years (e.g., a different shade instead of blue or another metal-based pigment for stability) can be distinguished by Raman Spectroscopy. When the elemental composition (e.g., Ti, Zn, Cr) changes yearly, this difference is seen in the EDX analysis [16].

This study aims to emphasize the importance of vehicle paints in terms of forensic science and to characterize paint residues that are considered trace evidence in crime scene investigations. Paint samples taken from vehicles of different brands, models, and production years were examined using FT-IR spectroscopy and SEM/EDX analysis methods, and the chemical and morphological properties of the paints were determined. It has been shown that even paints with similar colors can show differences. The study aims to contribute to future forensic practices to draw attention to the necessity of creating a reference database of vehicle paints in Türkiye.

MATERIAL AND METHODS

Reagents

Vehicle paint samples were obtained from the Çorum automobile industry zone. Among these samples, those suitable for examination were selected and examined in a laboratory environment. The samples were pulverized with a mechanical sanding machine and analyzed with FT-IR, and SEM/EDX images were taken. IR spectra were taken with the device in the chemistry department laboratory of Hitit University. SEM/EDX results were obtained through service procurement at Hitit University Scientific Technical and Application Research Center.

Table 1. Characteristics of the paint samples used in the research

Order	Vehicle brand	Production	Color
1	Renault Toros	1997	Blue
2	Volkswagen Polo	2014	Red
3	BMW 3	2016	White
4	Kia Sportage	2017	Gray
5	unknown	unknown	Red

Apparatus and instrumentation

Paint samples of five vehicles obtained from the auto industry zone were pulverized. Powdered samples were studied directly.

FT-IR Spectroscopy

IR spectroscopy was analyzed using a Fourier Transform Infrared Spectrometer (FT-IR) Thermo Scientific Nicolet 6700 device. FT-IR spectroscopy deals with the infrared region of the electromagnetic spectrum. Because each functional group consists of different atoms and bond strengths, the vibrations are specific to the functional group. FT-IR microspectrometers can be routinely applied in forensic samples because they are less costly and easy to use. Most paints exhibit strong absorbance between 1650 cm^{-1} and 1750 cm^{-1} (carbon-oxygen double bond stretching, sometimes a doublet for polyurethanes) and multiple absorbances (carbon-oxygen single bond stretching) between 1000 cm^{-1} and 1300 cm^{-1}. Although paints are quite complex, it is important to visually distinguish between simple acrylic, PVAc, polyurethane, and alkyd paints. Peaks at 815 cm^{-1} and 1550 cm^{-1} indicate the presence of melamine crosslinking [2].

Scanning Electron Microscope (SEM)

SEM analysis was made with Jeol JSM—5600, and EDX analysis was made with the FEI brand Quanta FEG 250 model. While performing EDX analyses, insulating vehicle paints were coated with gold-palladium coating and analyzed. Images with nanometer-scale resolution are produced and aid in interpretation. In the scanning electron microscope, the interaction between the electron beam and the material is used to obtain information from the sample's surface taken from living or non-living materials [17].

The sample is exposed to a high-energy electron beam in SEM, and the sample's morphology, topography, crystallographic information, etc., are determined. The most important problem at this stage is that electrons accumulate on the surface of the material taken, causing image loss, or the electron beam does not reflect sufficiently from the material. This problem is prevented by the coating materials used during sample preparation. Aluminum, gold, silver, palladium, and carbon can be used as coatings. The coating method prevents particularly sensitive materials from being damaged under the current generated by the electron beam.

RESULTS AND DISCUSSION

FT-IR Analyses

By referring to the relative intensity or shapes of certain absorption bands, the studied automobile paint samples were distinguished based on the Infrared spectra. The prominent peaks in the FT-IR spectrum of car paints, except for a few inorganic pigments, generally originate from the polymer binder. The FT-IR spectra of car paints are given in Figure 1, and the characteristic (diagnostic) bands in the infrared spectrum originating from the main polymer resins generally found in paint binders are given in Table 2. Modern automotive paint coatings commonly use amino resins, acrylic and/or alkyd resins in the top coat, polyurethanes and epoxy resins in the inner layers are used for corrosion protection, and it is well known that they contain crosslinking agents such as styrene [18]. While the paint in the top coat in the metal section consists of a styrene-acrylic-urethane polymer, the plastic section paint is a styrene-acrylic-melamine resin mixture. Therefore, one of the polymers that constitute the binder makes up the difference in chemical composition [18]. In the literature, the N–H Stretching peak observed for Urethane was determined as 3379 cm^{-1} and 3398 cm^{-1}, respectively, it was determined as 3548 cm^{-1} and 3406 cm^{-1} in the 1997 model Toros brand car [18]. The C=O (1724-1719 cm^{-1}) and C-O (1230 cm^{-1} - 1012 cm^{-1}) stretching peaks in the ester structure observed in almost all of the II, III, IV, and V numbered automobile paints given in Table 1 indicate the presence of acrylic and alkyd resins in the paint samples [18, 19, 20, 21]. The C=C stretching peaks detected as firm peaks at 1640 cm^{-1} and 1520 cm^{-1} in all paint samples (I-V) indicate Styrene and epoxy resins [19, 20, 21]. When the FT-IR spectrum of the unknown brand vehicle is examined, it is seen to have similar values to the Kia brand car. From here, we can guess that it may be a Kia brand or collided with a Kia brand vehicle.

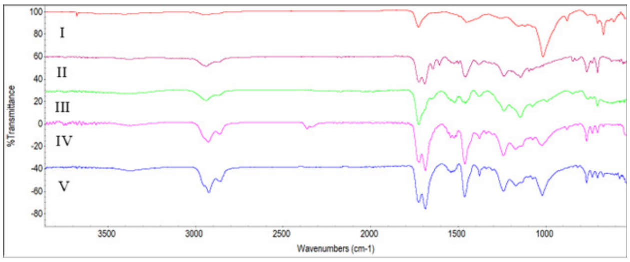

Figure 1. FT-IR spectra of cars. I. Renault Toros brand 1997 model blue colored car; II. Volkswagen Polo brand 2014 model red colored car; III. BMV 3 series brand 2016 model white colored car; IV. Kia Sportage brand 2017 model gray colored car; V. Red colored Unknown brand car

Table 2. FT-IR data of the vehicles (cm-1)

Complex	υ_{N-H}	υ_{O-H}	υ_{C-H}	$\upsilon_{C=O}$	$\upsilon_{C=C}$	$\upsilon_{C-H\ bending}$	υ_{C-O}
I	3548 3406	3354	2921 2854	1723 1683	1539	1460	1238 1016
II	-	3536	2932 2867	1724	1617	1452	1154 1012
III	-	3393	2936 2859	1722	1520	1456 1374	1236 1142
IV	-	3378	2935 2873	1722 1688	1640 1521	1456	1235 1141
V	-	3378	2924 2857	1719 1684	1521	1458	1238 1169

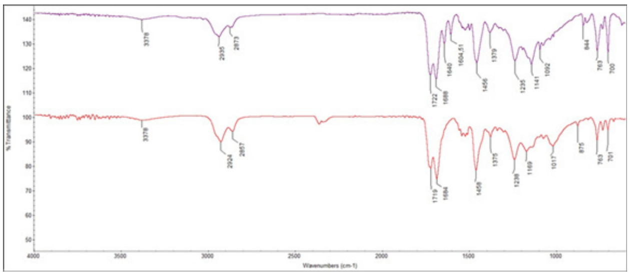

Figure 2. Spectra from top to bottom belong to the purple Volkswagen polo, and the red color belongs to the vehicle of an unknown brand and model.

SEM results

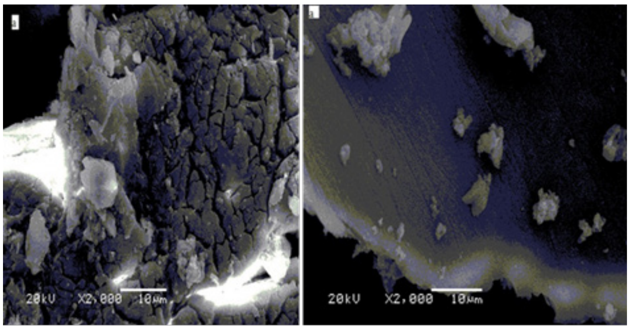

Picture 1. Electron microscope images of the blue paint of the Renault Toros brand, 1997 model, and Volkswagen Polo brand 2014 model red vehicle paint

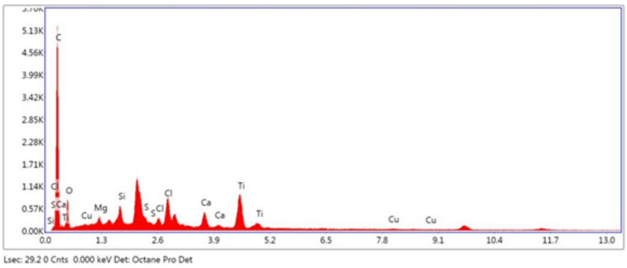

Figure 3. EDX results of Renault Toros brand 1997 model blue paint

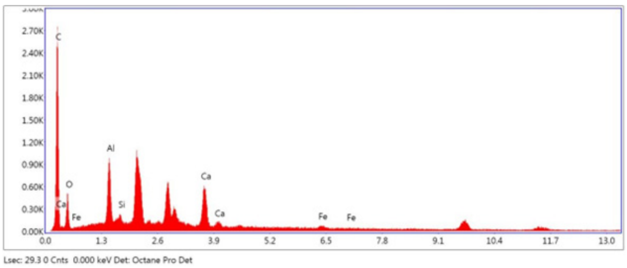

Figure 4. EDX results of Volkswagen Polo brand 2014 model red vehicle paint

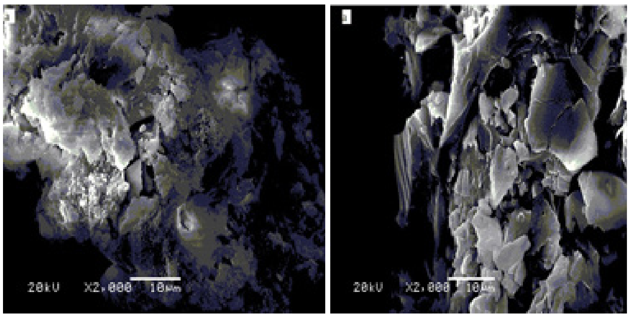

Picture 2. Electron microscope images of the white vehicle paint of the BMW 3 Series brand, 2016 model, and the gray paint of the 2017 model Kia Sportage

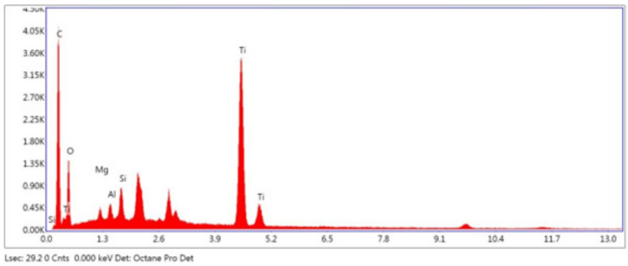

Figure 5. EDX results of BMW 3 Series brand 2016 model white vehicle paint

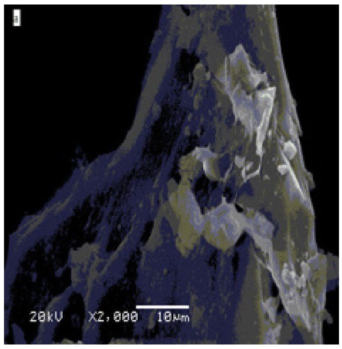

Picture 3. Electron microscope images of the red vehicle paint hitting a 2017 model gray Kia Sportage vehicle.

When the SEM results (Picture 1, Toros brand vehicle) are evaluated, the cracked and rough morphological structure can be seen in the first picture. The white and shiny appearance may be due to TiO_2 structured pigments. According to the EDX results in Figure 3, the presence of TiO_2 pigments is confirmed. C and O density shows that the paint content is highly organic. Detection of chlorine (Cl) and sulfur (S) elements may result from stabilizers, driers or chemical additives added to the paint system. According to the SEM image of the Volkswagen Polo vehicle in Picture 1, the surface has a wavy structure. As

Table 3. Elemental analysis results of Renault Toros, Volkswagen Polo, and BMW 3 Series vehicle paints

Order	Vehicle, model brand	Color	Production	Atomic Percentage of Elements									
				C	O	Al	Mg	Si	Ca	Ti	Fe	Cu	Cl
1	Renault Toros	Mavi	1997	68.23	16.58	-	0.41	1,16	1.88	6.38	-	0..40	0.68
2	Volkswagen Polo	Kırmızı	2014	65.29	22.44	4.76	-	0.35	6.81	-	0.35	-	-
3	BMW 3	Beyaz	2016	45.72	27.20	1.08	1.11	1.84	-	23.05	-	-	-

a result of the damage, a non-homogeneous, multilayered structure is formed. Silica or aluminum-based pigments or additives are available according to EDX (Figure 4). The SEM information of the BMW brand vehicle in Picture 2 shows fragmented, fractured, and porous areas on the surface. This can be seen when the paint peels off from the surface. When the SEM results of the red vehicle of an unknown model and brand that crashed into the Kia Sportage brand vehicle are examined, thin layers can be seen on the edges. Pointy-looking structures are related to brittle and cracked surfaces.

In this study, standard spectra were observed in the paint scales. The band seen at 1730 cm^{-1} is most likely from alkyd resins used in modern paints. Again, the bands observed around 3600 cm^{-1} and 1000 cm^{-1} in all paint samples indicate the presence of talc. Talc is a widely used filler in high-quality paint. Talc-filled compounds are common paint extenders due to their chemical inertness, allowing pigments to adhere to the vehicle surface and increasing durability. Alkyd resin is a widely used binder in the automotive industry. It is a synthetic resin made by a condensation reaction (water release) between a polyhydraulic alcohol and dibasic acid (phthalic anhydride). The polymer structure of alkyd resins makes them suitable for use as a base for enamels and paints with different specific properties. The structure molecules form strong structural interactions that include forming films that can cover any surface, providing protection against weathering and wear.

In our study, SEM images provided information about the surface topography of five paint samples. The red vehicle of an unknown brand that hit the 2017 model Kia Sportage is not the 2014 model red Volkswagen Polo we analyzed. We found that the FT-IR spectra and SEM images of the two-vehicle paints are different. As a result of the elemental analysis of the paints, the most common elements found in blue Renault Toros, red Volkswagen Polo, and white BMW 3 Series vehicles are C element, O element, and Si element. FT-IR results confirm the talc we found in the white BMW and the blue Renault Toros Mg and Si. The Fe element found in the red-colored Volkswagen indicates the presence of red iron oxide. The Ca element in Volkswagen Polo and Renault Toros vehicle paints may be related to calcium carbonate. Calcium carbonate has a tiny particle size. It is applied to protect the vehicle against impacts such as sand and gravel.

CONCLUSION

In this study, paint samples of five different vehicles were examined. It has been determined that the molecular structures of vehicle paints of different colors, brands, models, and production years are different. It has been determined that the microscopic images and FT-IR bands of two red vehicle paints that appear to be the same color are different. Epoxy and styrene resin were detected in all paint samples. SEM images provided information about the surface topography of the paint samples. Images: It has been shown that rough, cracked, and particle structures are present. According to the elemental analysis results, Ti, Si, Ca, and Al elements were found in the paint samples. Paint samples, one of the trace evidence frequently encountered in forensic cases, can be analyzed and used to create a paint database. Our study is planned to contribute to this issue.

Kochanowski (2000) analyzed and interpreted 100 vehicle paints in 5 colors with Py-GC-MS [22]. McIntee (2008) analyzed 110 automobile paints with LIBS (laser interactive plasma spectroscopy), FT-IR, and SEM/EDS and distinguished 88% of the samples [23]. Zieba-Palus (2010) examined 18 new and repainted solid and metallic paints [24]. Skenderovska et al. (2008) contributed to the police investigation by examining four different hit-and-run accidents with Raman and FT-IR spectrometers [25]. Gelder et al. (2005) analyzed paint flakes with Raman spectroscopy and evaluated their contributions to forensic science [26].

A study also shows that the new multimodal approach has a strong potential to elucidate the chemical and physical properties of multilayered vehicle paint particles and could be useful in detecting illegal vehicles. In this study, Fourier transforms infrared (ATR-FT-IR) imaging, Raman micro spectrometry (RMS), and scanning electron microscopy/energy dispersive X-ray spectrometric (SEM/EDX) techniques were performed in combination for detailed characterization of three car paint chip samples, providing complementary and comprehensive information about multilayer paint chips [6]. Maric et al. used FT-IR to characterize and evaluate the chemical diversity of electrocoating primer, primer surface coating, and base coats in automotive paint samples from 75 vehicles. Classification using principal component analysis revealed 14 distinct groups that could be correlated to country of manufacture, specific manufacturer and manufacturing facility, year of vehicle production, and in some cases, number of layers in the paint system [11]. Verma et al. (2019), in their study to distinguish automobile paint samples belonging to Maruti company in India, analyzed 20 paints with solubility tests and a UV spectrophotometer. In their study, unlike the literature, they worked on vehicle paints that had not been studied before. They observed the benefits of FT-IR and SEM analyses in hit-and-run situations with a high probability of paint chip change [27].

The paint particles detected in vehicle accidents are compared using global databases such as the number of layers, color pigments, FT-IR/UV-Vis spectra, and PDQ/EPG. With this study, we wanted to draw attention to the necessity of creating a reference database in order to make reliable comparisons in evaluating vehicle paints as trace evidence in forensic cases. Chemical and morphological analyses of paint samples from different vehicles reveal that each vehicle has its unique paint structure, and this brings up the need for a systematic archive to determine which vehicle the paint residues obtained from the scene belong to. Suppose a national vehicle paint database is created. In that case, it will be possible to identify vehicles through paint evidence in cases where there are no eyewitnesses or camera recordings, and it will make significant contributions to criminal investigations.

There is a need to create a vehicle paint database in our country. This study is intended to be a preliminary study for the vehicle paint database library that can be used in forensic sciences in our country in the future and to pioneer and contribute to new studies.

References

1. Hermens JGH, Gemert RV, Fringa BL. A coating from nature, Science Advances. 2020, 6, 51.
2. Kirkbride P. Paint and coatings examination. Forensic Chemistry Fundamentals and Applications. Editor: J.A. Siegel. Oxford, UK, 2016, 116-182.
3. Kaur S, Chauhan H, Kumar SS and Sunil A. Analysis of Unusual Trace Evidence- Paint & Glitter. Journal of Forensic Research. 2024, 15, 5.
4. Rendle DF. Advances in chemistry applied to forensic science. Chemical Society Reviews. 2005, 34, 1021-1030.
5. Brettell TA, Butler JM, Saferstein R. Forensic Science. Analytical Chemistry. 2005, 77, 3839-3860.
6. Malek MA, Nakazawa T, Kang HW, Tsuji K, Ro CU. Multi-modal Compositional Analysis of Layered Paint Chips of Automobiles by the Combined Application of ATR-FTIR Imaging, Raman Microspectrometry, and SEM/EDX. Molecules. 2019, 24(7):1381.
7. Karakaş F, Çelik MS. Stabilization mechanism of main paint pigments. Progress in Organic Coatings, 2018, 123, 292-298.
8. Koruyucu A. The Usage of Pigments In Textile Industry and Investigation of Their Effects on Human Health. İstanbul Commerce University Journal of Science. 2021, 20, (39) 146-161.
9. Suzuki, EM., Ryland, SG. Analysis of paint evidence. Forensic Chemistry Handbook. Editor: L. Kobilinsky. New Jersey. USA, 2012, 131-224.
10. Kumar, A. Exchange of paint in hit-run collisions and ıts significance as forensic evidence. Journal of Forensic Sciences. 2018, 8(1).
11. Maric, M, Bronswijk W, Lewis SW, Pitts K. Synchrotron FT-IR characterisation of automotive primer surface paint coatings for forensic purposes. Talanta 2014, 118, 156-161.
12. Thoonen, G, Nys, B, Haeghen, YV, Roy, GD, Scheunders P. Automatic forensic analysis of automotive paints using optical microscopy. Forensic Science İnternational 2016, 259, 210-220.
13. Hodgins T, Ho A, Sandercock M. Identification of Modern Automotive Paint Systems using Paint Data Query (PDQ): A Collaborative Study. Journal of the American Society of Trace Evidence Examiners. 2015, 6,3, 46-63.
14. Edinburgh Instruments. Forensic paint analysis using Raman microscopy. Retrieved from https://www.edinst.com/resource/forensic-paint-analysis-raman-microscopy/. 2024.
15. Duarte JM, Sales NGS, Sousa MH, Bridge C, Maric M, Gomes JA. Automotive paint analysis: How far has science advanced in the last ten years? TrAC Trends in Analytical Chemistry. 2020, 132, 116061.
16. Huang L, Beauchemin D. Forensic analysis of automotive paint chips for the vehicle manufacturer, color, and year of production using electrothermal vaporization coupled to inductively coupled plasma optical emission spectrometry. Journal of Analytical Atomic Spectrometry. 2017, 32(8).
17. Büken B, Üner B, Çetinkaya Ü, Çağdır AS, Kırangil ŞB. Scanning electron microscopy (SEM) applications in forensic medicine. Forensic Medicine Bulletin. 2001, 6, 1, 23-31.
18. Zięba-Palus, J. Examination of the variation of chemical composition and structure of paint within a car body by FT-IR and Raman spectroscopies. Journal of Molecular Structure 2020, 1219, 128558.
19. Verma, P, Kaur, N, Soni, P. Forensic evaluation and comparison of Indian automobile paint chips using FTIR. Materials Today: Proceedings 2020, 33, 1727–1732.
20. Özkınalı, S, Kocaokutgen, H. Synthesis, spectral characterization and thermal behaviors of some new p-tert-butylcalix[4]arene and calix[4]arene-esters containing acryloyl groups. Journal of Molecular Structure 2013, 1031, 70–78.
21. Özkınalı, S. Spectroscopic, and thermal properties of newly mixed azocalix[4]arene ester derivatives. Dyes and Pigments 2014, 107, 81–89.
22. Kochanowski, BK, Morgan, SL. Forensıc discrimination of automotive paint samples using pyrolysis-gas chromatography-mass spectrometry with multivariate statistics. Journal of Chromatographic Science, 2000, 38(3):100-8.
23. McIntee, EM. Forensic analysis of automobile paints by atomic and molecular spectroscopic methods and statical data analyses. Degree of Master of Science in the Department of Chemistry in the College of Sciences at the University of Central Florida Orlando, 2002, Florida.
24. Zieba-Palus, J, Koscielniak P. Comparative analysis of car paint traces in terms of color by VIS micro spectrometry for forensic needs. Analytical Letters. 2010, 43(3), 436-445.
25. Skenderovska, M, Sukarova BM, Andreeva, L. Application of mıcro-Raman and FT-IR spectroscopy in forensic analıysıs of automotive topcoats in the republıc of Macedonia. Macedonian Journal of Chemistry and Chemical Engineering. 2008, 27,1.
26. Gelder, JD, Vandenabeele P, Govaert F, Moens L. Forensıc analysis of automotive paints by Raman spectroscopy. Journal of Raman Spectroscopy, 2005, 36, 1059-1067.
27. Verma P, Kaur M, Kaur N. Forensic analysis of automobile paint of Indian company. Int J Forensic Med Toxicol Sci 2019;4(3):74-81.